Eur. Phys. J. C (2018) 78:165
https://doi.org/10.1140/epjc/s10052-018-5567-9

THE EUROPEAN PHYSICAL JOURNAL C

Regular Article - Experimental Physics

Measurements of the pp → ZZ production cross section and the Z → 4ℓ branching fraction, and constraints on anomalous triple gauge couplings at $\sqrt{s} = 13$ TeV

CMS Collaboration*

CERN, 1211 Geneva 23, Switzerland

Received: 25 September 2017 / Accepted: 17 January 2018

Abstract Four-lepton production in proton-proton collisions, pp → $(Z/\gamma^*)(Z/\gamma^*)$ → 4ℓ, where ℓ = e or μ, is studied at a center-of-mass energy of 13 TeV with the CMS detector at the LHC. The data sample corresponds to an integrated luminosity of 35.9 fb^{-1}. The ZZ production cross section, $\sigma(pp \to ZZ) = 17.2 \pm 0.5\,(stat) \pm 0.7\,(syst) \pm 0.4\,(theo) \pm 0.4\,(lumi)$ pb, measured using events with two opposite-sign, same-flavor lepton pairs produced in the mass region $60 < m_{\ell^+\ell^-} < 120$ GeV, is consistent with standard model predictions. Differential cross sections are measured and are well described by the theoretical predictions. The Z boson branching fraction to four leptons is measured to be $\mathcal{B}(Z \to 4\ell) = 4.83^{+0.23}_{-0.22}(stat)^{+0.32}_{-0.29}(syst) \pm 0.08(theo) \pm 0.12(lumi) \times 10^{-6}$ for events with a four-lepton invariant mass in the range $80 < m_{4\ell} < 100$ GeV and a dilepton mass $m_{\ell\ell} > 4$ GeV for all opposite-sign, same-flavor lepton pairs. The results agree with standard model predictions. The invariant mass distribution of the four-lepton system is used to set limits on anomalous ZZZ and ZZγ couplings at 95% confidence level: $-0.0012 < f_4^Z < 0.0010$, $-0.0010 < f_5^Z < 0.0013$, $-0.0012 < f_4^\gamma < 0.0013$, $-0.0012 < f_5^\gamma < 0.0013$.

1 Introduction

Measurements of diboson production at the CERN LHC allow precision tests of the standard model (SM). In the SM, ZZ production proceeds mainly through quark-antiquark t- and u-channel scattering diagrams. In calculations at higher orders in quantum chromodynamics (QCD), gluon-gluon fusion also contributes via box diagrams with quark loops. There are no tree-level contributions to ZZ production from triple gauge boson vertices in the SM. Anomalous triple gauge couplings (aTGC) could be induced by new physics models such as supersymmetry [1]. Nonzero aTGCs may be parametrized using an effective Lagrangian as in Ref. [2]. In this formalism, two ZZZ and two ZZγ couplings are allowed by electromagnetic gauge invariance and Lorentz invariance for on-shell Z bosons. These are described by two CP-violating (f_4^V) and two CP-conserving (f_5^V) parameters, where V = Z or γ.

Previous measurements of the ZZ production cross section by the CMS Collaboration were performed for pairs of on-shell Z bosons, produced in the dilepton mass range 60–120 GeV [3–6]. These measurements were made with data sets corresponding to integrated luminosities of 5.1 fb^{-1} at $\sqrt{s} = 7$ TeV and 19.6 fb^{-1} at $\sqrt{s} = 8$ TeV in the ZZ → 2ℓ2ℓ″ and ZZ → 2ℓ2ν decay channels, where ℓ = e or μ and ℓ″ = e, μ, or τ, and with an integrated luminosity of 2.6 fb^{-1} at $\sqrt{s} = 13$ TeV in the ZZ → 2ℓ2ℓ′ decay channel, where ℓ′ = e or μ. All of them agree with SM predictions. The ATLAS Collaboration produced similar results at $\sqrt{s} = 7$, 8, and 13 TeV [7–10], which also agree with the SM. These measurements are important for testing predictions that were recently made available at next-to-next-to-leading order (NNLO) in QCD [11]. Comparing these predictions with data at a range of center-of-mass energies provides information about the electroweak gauge sector of the SM. Because the uncertainty of the CMS measurement at $\sqrt{s} = 13$ TeV [6] was dominated by the statistical uncertainty of the observed data, repeating and extending the measurement with a larger sample of proton-proton collision data at $\sqrt{s} = 13$ TeV improves the precision of the results.

The most stringent previous limits on ZZZ and ZZγ aTGCs from CMS were set using the 7 and 8 TeV data samples: $-0.0022 < f_4^Z < 0.0026$, $-0.0023 < f_5^Z < 0.0023$, $-0.0029 < f_4^\gamma < 0.0026$, and $-0.0026 < f_5^\gamma < 0.0027$ at 95% confidence level (CL) [4,5]. Similar limits were obtained by the ATLAS Collaboration [12], who also recently produced limits using 13 TeV data [10].

Extending the dilepton mass range to lower values allows measurements of $(Z/\gamma^*)\,(Z/\gamma^*)$ production, where Z indi-

* e-mail: cms-publication-committee-chair@cern.ch

Published online: 24 February 2018

cates an on-shell Z boson or an off-shell Z* boson. The resulting sample includes Higgs boson events in the $H \to ZZ^* \to 2\ell 2\ell'$ channel, and rare decays of a single Z boson to four leptons. The $Z \to \ell^+\ell^-\gamma^* \to 2\ell 2\ell'$ decay was studied in detail at LEP [13] and was observed in pp collisions by CMS [6,14] and ATLAS [15]. Although the branching fraction for this decay is orders of magnitude smaller than that for the $Z \to \ell^+\ell^-$ decay, the precisely known mass of the Z boson makes the four-lepton mode useful for calibrating mass measurements of the nearby Higgs boson resonance.

This paper reports a study of four-lepton production ($pp \to 2\ell 2\ell'$, where 2ℓ and $2\ell'$ indicate opposite-sign pairs of electrons or muons) at $\sqrt{s} = 13$ TeV with a data set corresponding to an integrated luminosity of $35.9 \pm 0.9\,\text{fb}^{-1}$ recorded in 2016. Cross sections are measured for nonresonant production of pairs of Z bosons, $pp \to ZZ$, where both Z bosons are produced on-shell, defined as the mass range 60–120 GeV, and resonant $pp \to Z \to 4\ell$ production. Detailed discussion of resonant Higgs boson production decaying to ZZ*, is beyond the scope of this paper and may be found in Ref. [16].

2 The CMS detector

A detailed description of the CMS detector, together with a definition of the coordinate system used and the relevant kinematic variables, can be found in Ref. [17].

The central feature of the CMS apparatus is a superconducting solenoid of 6 m internal diameter, providing a magnetic field of 3.8 T. Within the solenoid volume are a silicon pixel and strip tracker, a lead tungstate crystal electromagnetic calorimeter (ECAL), and a brass and scintillator hadron calorimeter, which provide coverage in pseudorapidity $|\eta| < 1.479$ in a cylindrical barrel and $1.479 < |\eta| < 3.0$ in two endcap regions. Forward calorimeters extend the coverage provided by the barrel and endcap detectors to $|\eta| < 5.0$. Muons are measured in gas-ionization detectors embedded in the steel flux-return yoke outside the solenoid in the range $|\eta| < 2.4$, with detection planes made using three technologies: drift tubes, cathode strip chambers, and resistive plate chambers.

Electron momenta are estimated by combining energy measurements in the ECAL with momentum measurements in the tracker. The momentum resolution for electrons with transverse momentum $p_T \approx 45$ GeV from $Z \to e^+e^-$ decays ranges from 1.7% for nonshowering electrons in the barrel region to 4.5% for showering electrons in the endcaps [18]. Matching muons to tracks identified in the silicon tracker results in a p_T resolution for muons with $20 < p_T < 100$ GeV of 1.3–2.0% in the barrel and better than 6% in the endcaps. The p_T resolution in the barrel is better than 10% for muons with p_T up to 1 TeV [19].

3 Signal and background simulation

Signal events are generated with POWHEG 2.0 [20–24] at next-to-leading order (NLO) in QCD for quark-antiquark processes and leading order (LO) for quark-gluon processes. This includes ZZ, $Z\gamma^*$, Z, and $\gamma^*\gamma^*$ production with a constraint of $m_{\ell\ell'} > 4$ GeV applied to all pairs of oppositely charged leptons at the generator level to avoid infrared divergences. The $gg \to ZZ$ process is simulated at LO with MCFM v7.0 [25]. These samples are scaled to correspond to cross sections calculated at NNLO in QCD for $q\bar{q} \to ZZ$ [11] (a scaling K factor of 1.1) and at NLO in QCD for $gg \to ZZ$ [26] (K factor of 1.7). The $gg \to ZZ$ process is calculated to $\mathcal{O}\left(\alpha_s^3\right)$, where α_s is the strong coupling constant, while the other contributing processes are calculated to $\mathcal{O}\left(\alpha_s^2\right)$; this higher-order correction is included because the effect is known to be large [26]. Electroweak ZZ production in association with two jets is generated with PHANTOM v1.2.8 [27].

A sample of Higgs boson events is produced in the gluon-gluon fusion process at NLO with POWHEG. The Higgs boson decay is modeled with JHUGEN 3.1.8 [28–30]. Its cross section is scaled to the NNLO prediction with a K factor of 1.7 [26].

Samples for background processes containing four prompt leptons in the final state, $t\bar{t}Z$ and WWZ production, are produced with MADGRAPH5_aMC@NLO v2.3.3 [31]. The $q\bar{q} \to WZ$ process is generated with POWHEG.

Samples with aTGC contributions included are generated at LO with SHERPA v2.1.1 [32]. Distributions from the SHERPA samples are normalized such that the total yield of the SM sample is the same as that of the POWHEG sample.

The PYTHIA v8.175 [23,33,34] package is used for parton showering, hadronization, and the underlying event simulation, with parameters set by the CUETP8M1 tune [35], for all samples except the samples generated with SHERPA, which performs these functions itself. The NNPDF 3.0 [36] set is used as the default set of parton distribution functions (PDFs). For all simulated event samples, the PDFs are calculated to the same order in QCD as the process in the sample.

The detector response is simulated using a detailed description of the CMS detector implemented with the GEANT4 package [37]. The event reconstruction is performed with the same algorithms used for data. The simulated samples include additional interactions per bunch crossing, referred to as pileup. The simulated events are weighted so that the pileup distribution matches the data, with an average of about 27 interactions per bunch crossing.

4 Event reconstruction

All long-lived particles—electrons, muons, photons, and charged and neutral hadrons—in each collision event are

identified and reconstructed with the CMS particle-flow (PF) algorithm [38] from a combination of the signals from all subdetectors. Reconstructed electrons [18] and muons [19] are considered candidates for inclusion in four-lepton final states if they have $p_{\mathrm{T}}^{\mathrm{e}} > 7\,\mathrm{GeV}$ and $|\eta^{\mathrm{e}}| < 2.5$ or $p_{\mathrm{T}}^{\mu} > 5\,\mathrm{GeV}$ and $|\eta^{\mu}| < 2.4$.

Lepton candidates are also required to originate from the event vertex, defined as the reconstructed proton-proton interaction vertex with the largest value of summed physics object p_{T}^2. The physics objects used in the event vertex definition are the objects returned by a jet finding algorithm [39,40] applied to all charged tracks associated with the vertex, plus the corresponding associated missing transverse momentum [41]. The distance of closest approach between each lepton track and the event vertex is required to be less than 0.5 cm in the plane transverse to the beam axis, and less than 1 cm in the direction along the beam axis. Furthermore, the significance of the three-dimensional impact parameter relative to the event vertex, $\mathrm{SIP_{3D}}$, is required to satisfy $\mathrm{SIP_{3D}} \equiv |\mathrm{IP}/\sigma_{\mathrm{IP}}| < 10$ for each lepton, where IP is the distance of closest approach of each lepton track to the event vertex and σ_{IP} is its associated uncertainty.

Lepton candidates are required to be isolated from other particles in the event. The relative isolation is defined as

$$R_{\mathrm{iso}} = \left[\sum_{\substack{\text{charged}\\ \text{hadrons}}} p_{\mathrm{T}} + \max\left(0, \sum_{\substack{\text{neutral}\\ \text{hadrons}}} p_{\mathrm{T}} + \sum_{\text{photons}} p_{\mathrm{T}} - p_{\mathrm{T}}^{\mathrm{PU}}\right)\right] \Big/ p_{\mathrm{T}}^{\ell}, \tag{1}$$

where the sums run over the charged and neutral hadrons and photons identified by the PF algorithm, in a cone defined by $\Delta R \equiv \sqrt{(\Delta\eta)^2 + (\Delta\phi)^2} < 0.3$ around the lepton trajectory. Here ϕ is the azimuthal angle in radians. To minimize the contribution of charged particles from pileup to the isolation calculation, charged hadrons are included only if they originate from the event vertex. The contribution of neutral particles from pileup is $p_{\mathrm{T}}^{\mathrm{PU}}$. For electrons, $p_{\mathrm{T}}^{\mathrm{PU}}$ is evaluated with the "jet area" method described in Ref. [42]; for muons, it is taken to be half the sum of the p_{T} of all charged particles in the cone originating from pileup vertices. The factor one-half accounts for the expected ratio of charged to neutral particle energy in hadronic interactions. A lepton is considered isolated if $R_{\mathrm{iso}} < 0.35$.

The lepton reconstruction, identification, and isolation efficiencies are measured with a "tag-and-probe" technique [43] applied to a sample of $\mathrm{Z} \to \ell^+\ell^-$ data events. The measurements are performed in several bins of p_{T}^{ℓ} and $|\eta^{\ell}|$. The electron reconstruction and selection efficiency in the ECAL barrel (endcaps) varies from about 85% (77%) at $p_{\mathrm{T}}^{\mathrm{e}} \approx 10\,\mathrm{GeV}$ to about 95% (89%) for $p_{\mathrm{T}}^{\mathrm{e}} \geq 20\,\mathrm{GeV}$, while in the barrel-endcap transition region this efficiency is about 85% averaged over all electrons with $p_{\mathrm{T}}^{\mathrm{e}} > 7\,\mathrm{GeV}$. The muons are reconstructed and identified with efficiencies above $\sim 98\%$ within $|\eta^{\mu}| < 2.4$.

5 Event selection

The primary triggers for this analysis require the presence of a pair of loosely isolated leptons of the same or different flavors [44]. The highest p_{T} lepton must have $p_{\mathrm{T}}^{\ell} > 17\,\mathrm{GeV}$, and the subleading lepton must have $p_{\mathrm{T}}^{\mathrm{e}} > 12\,\mathrm{GeV}$ if it is an electron or $p_{\mathrm{T}}^{\mu} > 8\,\mathrm{GeV}$ if it is a muon. The tracks of the triggering leptons are required to originate within 2 mm of each other in the plane transverse to the beam axis. Triggers requiring a triplet of lower-p_{T} leptons with no isolation criterion, or a single high-p_{T} electron or muon, are also used. An event is used if it passes any trigger regardless of the decay channel. The total trigger efficiency for events within the acceptance of this analysis is greater than 98%.

The four-lepton candidate selections are based on those used in Ref. [45]. A signal event must contain at least two Z/γ^* candidates, each formed from an oppositely charged pair of isolated electron candidates or muon candidates. Among the four leptons, the highest p_{T} lepton must have $p_{\mathrm{T}} > 20\,\mathrm{GeV}$, and the second-highest p_{T} lepton must have $p_{\mathrm{T}}^{\mathrm{e}} > 12\,\mathrm{GeV}$ if it is an electron or $p_{\mathrm{T}}^{\mu} > 10\,\mathrm{GeV}$ if it is a muon. All leptons are required to be separated from each other by $\Delta R\,(\ell_1, \ell_2) > 0.02$, and electrons are required to be separated from muons by $\Delta R\,(\mathrm{e}, \mu) > 0.05$.

Within each event, all permutations of leptons giving a valid pair of Z/γ^* candidates are considered separately. Within each 4ℓ candidate, the dilepton candidate with an invariant mass closest to 91.2 GeV, taken as the nominal Z boson mass [46], is denoted $\mathrm{Z_1}$ and is required to have a mass greater than 40 GeV. The other dilepton candidate is denoted $\mathrm{Z_2}$. Both $m_{\mathrm{Z_1}}$ and $m_{\mathrm{Z_2}}$ are required to be less than 120 GeV. All pairs of oppositely charged leptons in the 4ℓ candidate are required to have $m_{\ell\ell'} > 4\,\mathrm{GeV}$ regardless of their flavor.

If multiple 4ℓ candidates within an event pass all selections, the one with $m_{\mathrm{Z_1}}$ closest to the nominal Z boson mass is chosen. In the rare case of further ambiguity, which may arise in less than 0.5% of events when five or more passing lepton candidates are found, the $\mathrm{Z_2}$ candidate that maximizes the scalar p_{T} sum of the four leptons is chosen.

Additional requirements are applied to select events for measurements of specific processes. The $\mathrm{pp} \to \mathrm{ZZ}$ cross section is measured using events where both $m_{\mathrm{Z_1}}$ and $m_{\mathrm{Z_2}}$ are greater than 60 GeV. The $\mathrm{Z} \to 4\ell$ branching fraction is measured using events with $80 < m_{4\ell} < 100\,\mathrm{GeV}$, a range chosen to retain most of the decays in the resonance while removing most other processes with four-lepton final states. Decays of the Z bosons to τ leptons with subsequent decays to electrons and muons are heavily suppressed by requirements on lepton p_{T}, and the contribution of such events is

less than 0.5% of the total ZZ yield. If these events pass the selection requirements of the analysis, they are considered signal, while they are not considered at generator level in the cross section unfolding procedure. Thus, the correction for possible τ decays is included in the efficiency calculation.

6 Background estimate

The major background contributions arise from Z boson and WZ diboson production in association with jets and from $\mathrm{t\bar{t}}$ production. In all these cases, particles from jet fragmentation satisfy both lepton identification and isolation criteria, and are thus misidentified as signal leptons.

The probability for such objects to be selected is measured from a sample of $\mathrm{Z} + \ell_{\text{candidate}}$ events, where Z denotes a pair of oppositely charged, same-flavor leptons that pass all analysis requirements and satisfy $|m_{\ell^+\ell^-} - m_{\mathrm{Z}}| < 10\,\text{GeV}$, where m_{Z} is the nominal Z boson mass. Each event in this sample must have exactly one additional object $\ell_{\text{candidate}}$ that passes relaxed identification requirements with no isolation requirements applied. The misidentification probability for each lepton flavor, measured in bins of lepton candidate p_{T} and η, is defined as the ratio of the number of candidates that pass the final isolation and identification requirements to the total number in the sample. The number of $\mathrm{Z} + \ell_{\text{candidate}}$ events is corrected for the contamination from WZ production and ZZ production in which one lepton is not reconstructed. These events have a third genuine, isolated lepton that must be excluded from the misidentification probability calculation. The WZ contamination is suppressed by requiring the missing transverse momentum $p_{\mathrm{T}}^{\text{miss}}$ to be below 25 GeV. The $p_{\mathrm{T}}^{\text{miss}}$ is defined as the magnitude of the missing transverse momentum vector $\vec{p}_{\mathrm{T}}^{\,\text{miss}}$, the projection onto the plane transverse to the beams of the negative vector sum of the momenta of all reconstructed PF candidates in the event, corrected for the jet energy scale. Additionally, the transverse mass calculated with $\vec{p}_{\mathrm{T}}^{\,\text{miss}}$ and the $\vec{p}_{\mathrm{T}}$ of $\ell_{\text{candidate}}$, $m_{\mathrm{T}} \equiv \sqrt{(p_{\mathrm{T}}^{\ell} + p_{\mathrm{T}}^{\text{miss}})^2 - (\vec{p}_{\mathrm{T}}^{\,\ell} + \vec{p}_{\mathrm{T}}^{\,\text{miss}})^2}$, is required to be less than 30 GeV. The residual contribution of WZ and ZZ events, which may be up to a few percent of the events with $\ell_{\text{candidate}}$ passing all selection criteria, is estimated from simulation and subtracted.

To account for all sources of background events, two control samples are used to estimate the number of background events in the signal regions. Both are defined to contain events with a dilepton candidate satisfying all requirements ($\mathrm{Z_1}$) and two additional lepton candidates $\ell'^{+}\ell'^{-}$. In one control sample, enriched in WZ events, one ℓ' candidate is required to satisfy the full identification and isolation criteria and the other must fail the full criteria and instead satisfy only the relaxed ones; in the other, enriched in Z+jets events, both ℓ' candidates must satisfy the relaxed criteria, but fail the full criteria. The additional leptons must have opposite charge and the same flavor ($\mathrm{e^{\pm}e^{\mp}}$, $\mu^{\pm}\mu^{\mp}$). From this set of events, the expected number of background events in the signal region, denoted "Z + X" in the figures, is obtained by scaling the number of observed $\mathrm{Z_1} + \ell'^{+}\ell'^{-}$ events by the misidentification probability for each lepton failing the selection. It is found to be approximately 4% of the total expected yield. The procedure is described in more detail in Ref. [45].

In addition to these nonprompt backgrounds, $\mathrm{t\bar{t}Z}$ and WWZ processes contribute a smaller number of events with four prompt leptons, which is estimated from simulated samples to be around 1% of the expected $\mathrm{ZZ} \to 4\ell$ yield. In the $\mathrm{Z} \to 4\ell$ selection, the contribution from these backgrounds is negligible. The total background contributions to the $\mathrm{Z} \to 4\ell$ and $\mathrm{ZZ} \to 4\ell$ signal regions are summarized in Sect. 8.

7 Systematic uncertainties

The major sources of systematic uncertainty and their effect on the measured cross sections are summarized in Table 1. In both data and simulated event samples, trigger efficiencies are evaluated with a tag-and-probe technique. The ratio of data to simulation is applied to simulated events, and the size of the resulting change in expected yield is taken as the uncertainty in the determination of the trigger efficiency. This uncertainty is around 2% of the final estimated yield. For $\mathrm{Z} \to 4\mathrm{e}$ events, the uncertainty increases to 4%.

The lepton identification, isolation, and track reconstruction efficiencies in simulation are corrected with scaling factors derived with a tag-and-probe method and applied as a function of lepton p_{T} and η. To estimate the uncertainties associated with the tag-and-probe technique, the total yield

Table 1 The contributions of each source of systematic uncertainty in the cross section measurements. The integrated luminosity uncertainty, and the PDF and scale uncertainties, are considered separately. All other uncertainties are added in quadrature into a single systematic uncertainty. Uncertainties that vary by decay channel are listed as a range

Uncertainty	$\mathrm{Z} \to 4\ell$ (%)	$\mathrm{ZZ} \to 4\ell$ (%)
Lepton efficiency	6–10	2–6
Trigger efficiency	2–4	2
Statistical (simulation)	1–2	0.5
Background	0.6–1.3	0.5–1
Pileup	1–2	1
PDF	1	1
μ_{R}, μ_{F}	1	1
Integrated luminosity	2.5	2.5

is recomputed with the scaling factors varied up and down by the tag-and-probe fit uncertainties. The uncertainties associated with lepton efficiency in the ZZ $\to 4\ell$ (Z $\to 4\ell$) signal regions are found to be 6(10)% in the 4e, 3(6)% in the 2e2μ, and 2(7)% in the 4μ final states. These uncertainties are higher for Z $\to 4\ell$ events because the leptons generally have lower p_{T}, and the samples used in the tag-and-probe method have fewer events and more contamination from nonprompt leptons in this low-p_{T} region.

Uncertainties due to the effect of factorization (μ_{F}) and renormalization (μ_{R}) scale choices on the ZZ $\to 4\ell$ acceptance are evaluated with POWHEG and MCFM by varying the scales up and down by a factor of two with respect to the default values $\mu_{\mathrm{F}} = \mu_{\mathrm{R}} = m_{\mathrm{ZZ}}$. All combinations are considered except those in which μ_{F} and μ_{R} differ by a factor of four. Parametric uncertainties (PDF + α_s) are evaluated according to the PDF4LHC prescription [47] in the acceptance calculation, and with NNPDF3.0 in the cross section calculations. An additional theoretical uncertainty arises from scaling the POWHEG $\mathrm{q\bar{q}} \to$ ZZ simulated sample from its NLO cross section to the NNLO prediction, and the MCFM gg $\to$ ZZ samples from their LO cross sections to the NLO predictions. The change in the acceptance corresponding to this scaling procedure is found to be 1.1%. All these theoretical uncertainties are added in quadrature.

The largest uncertainty in the estimated background yield arises from differences in sample composition between the Z + $\ell_{\mathrm{candidate}}$ control sample used to calculate the lepton misidentification probability and the Z + $\ell^+\ell^-$ control sample. A further uncertainty arises from the limited number of events in the Z + $\ell_{\mathrm{candidate}}$ sample. A systematic uncertainty of 40% is applied to the lepton misidentification probability to cover both effects. The size of this uncertainty varies by channel, but is less than 1% of the total expected yield.

The uncertainty in the integrated luminosity of the data sample is 2.5% [48].

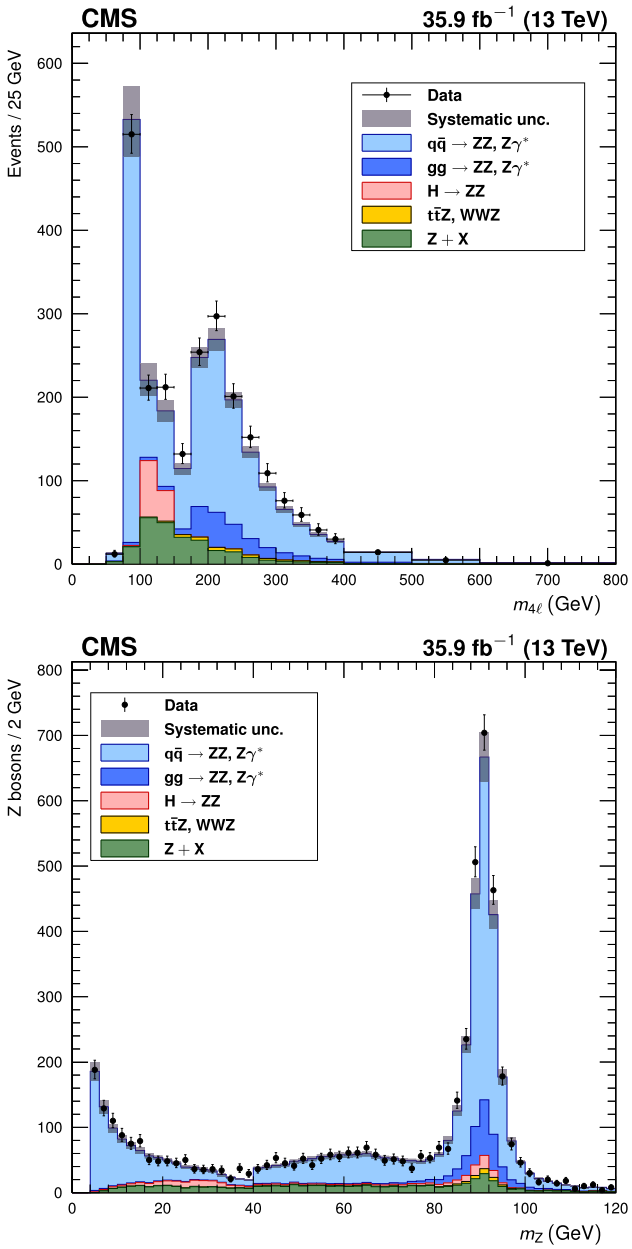

Fig. 1 Distributions of (upper) the four-lepton invariant mass $m_{4\ell}$ and (lower) the dilepton invariant mass of all Z/γ^* bosons in selected four-lepton events. Both selected dilepton candidates are included in each event. In the $m_{4\ell}$ distribution, bin contents are normalized to a bin width of 25 GeV; horizontal bars on the data points show the range of the corresponding bin. Points represent the data, while filled histograms represent the SM prediction and background estimate. Vertical bars on the data points show their statistical uncertainty. Shaded grey regions around the predicted yield represent combined statistical, systematic, theoretical, and integrated luminosity uncertainties

8 Cross section measurements

The distributions of the four-lepton mass and the masses of the Z_1 and Z_2 candidates are shown in Fig. 1. The expected distributions describe the data well within uncertainties. The SM predictions include nonresonant ZZ predictions, production of the SM Higgs boson with mass 125 GeV [49], and resonant Z $\to 4\ell$ production. The backgrounds estimated from data and simulation are also shown. The reconstructed invariant mass of the Z_1 candidates, and a scatter plot showing the correlation between m_{Z_2} and m_{Z_1} in data events, are shown in Fig. 2. In the scatter plot, clusters of events corresponding to ZZ $\to 4\ell$, Z$\gamma^* \to 4\ell$, and Z $\to 4\ell$ production can be seen.

The four-lepton invariant mass distribution below 100 GeV is shown in Fig. 3 (upper). Figure 3 (lower) shows m_{Z_2} plotted against m_{Z_1} for events with $m_{4\ell}$ between 80 and 100 GeV, and the observed and expected event yields in this mass region are given in Table 2. The yield of events in the 4e final state

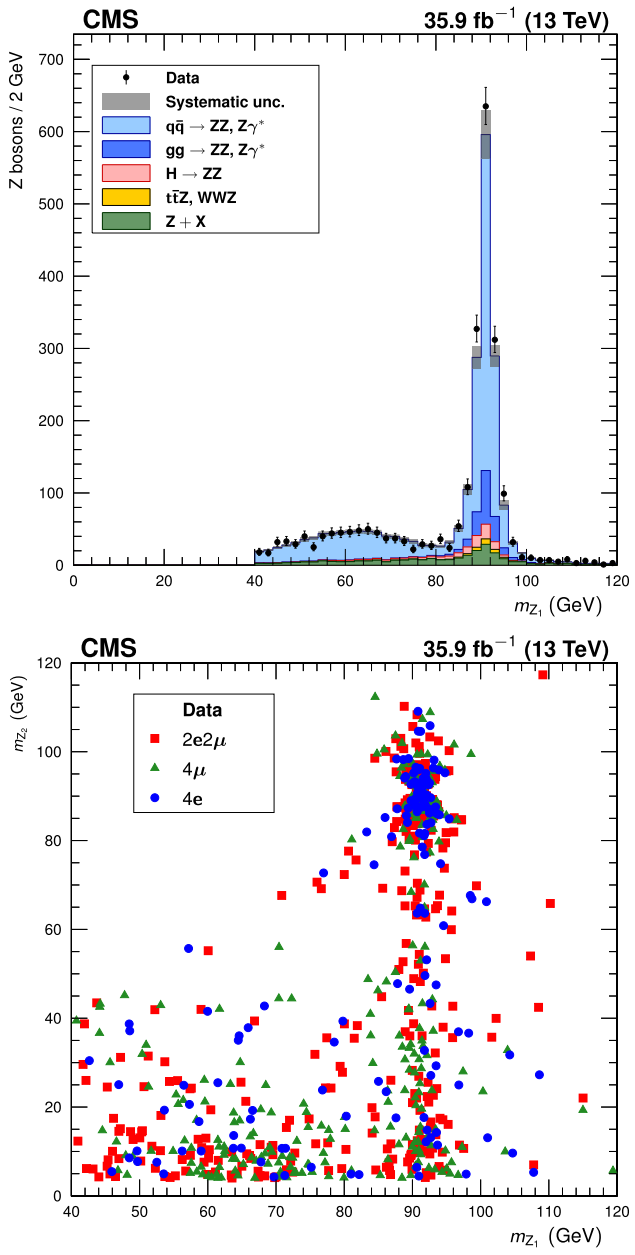

Fig. 2 (Upper): the distribution of the reconstructed mass of Z_1, the dilepton candidate closer to the nominal Z boson mass. Points represent the data, while filled histograms represent the SM prediction and background estimate. Vertical bars on the data points show their statistical uncertainty. Shaded grey regions around the predicted yield represent combined statistical, systematic, theoretical, and integrated luminosity uncertainties. (Lower): the reconstructed m_{Z_2} plotted against the reconstructed m_{Z_1} in data events, with distinctive markers for each final state. For readability, only every fourth event is plotted

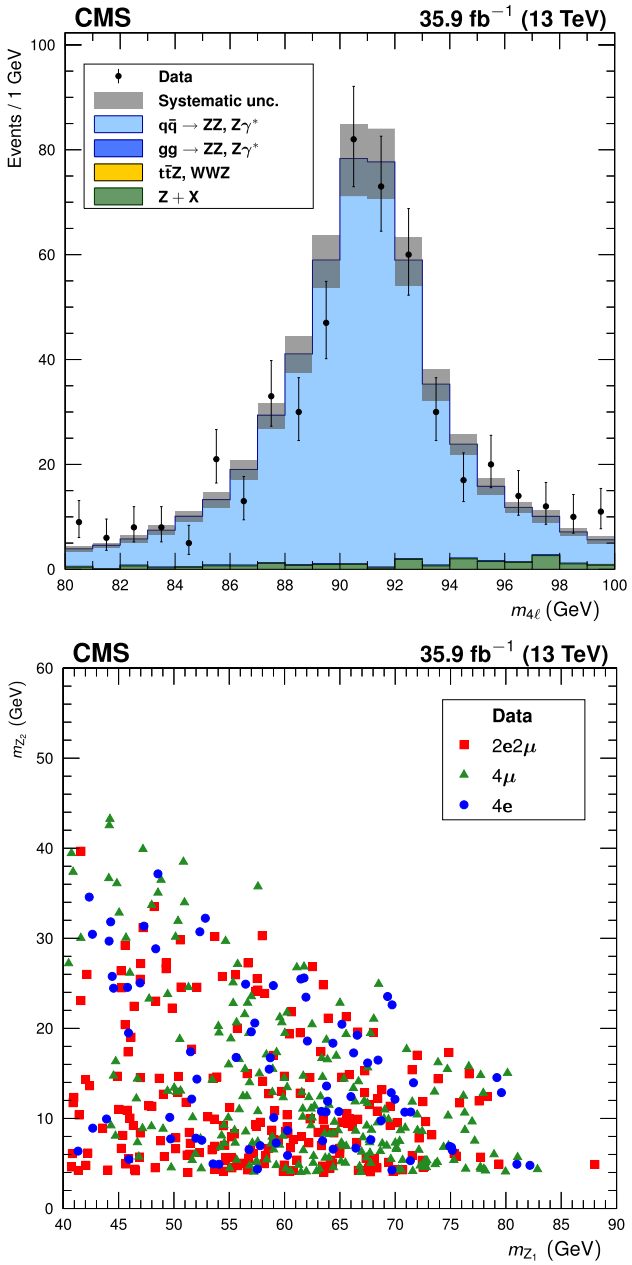

Fig. 3 (Upper): the distribution of the reconstructed four-lepton mass $m_{4\ell}$ for events selected with $80 < m_{4\ell} < 100$ GeV. Points represent the data, while filled histograms represent the SM prediction and background estimate. Vertical bars on the data points show their statistical uncertainty. Shaded grey regions around the predicted yield represent combined statistical, systematic, theoretical, and integrated luminosity uncertainties. (Lower): the reconstructed m_{Z_2} plotted against the reconstructed m_{Z_1} for all data events selected with $m_{4\ell}$ between 80 and 100 GeV, with distinctive markers for each final state

is significantly lower than in the 4μ final state because minimum p_T thresholds are higher for electrons than for muons, and inefficiencies in the detection of low-p_T leptons affect electrons more strongly than they affect muons.

The reconstructed four-lepton invariant mass is shown in Fig. 4 (upper) for events with two on-shell Z bosons. Figure 4 (lower) shows the invariant mass distribution for all Z boson candidates in these events. The corresponding observed and expected yields are given in Table 3.

The observed yields are used to evaluate the $pp \to Z \to 4\ell$ and $pp \to ZZ \to 4\ell$ production cross sections from a

Table 2 The observed and expected yields of four-lepton events in the mass region $80 < m_{4\ell} < 100$ GeV and estimated yields of background events, shown for each final state and summed in the total expected yield. The first uncertainty is statistical, the second one is systematic. The systematic uncertainties do not include the uncertainty in the integrated luminosity

Final state	Expected $N_{4\ell}$	Background	Total expected	Observed
4μ	$224 \pm 1 \pm 16$	$7 \pm 1 \pm 2$	$231 \pm 2 \pm 17$	225
$2e2\mu$	$207 \pm 1 \pm 14$	$9 \pm 1 \pm 2$	$216 \pm 2 \pm 14$	206
4e	$68 \pm 1 \pm 8$	$4 \pm 1 \pm 2$	$72 \pm 1 \pm 8$	78
Total	$499 \pm 2 \pm 32$	$19 \pm 2 \pm 5$	$518 \pm 3 \pm 33$	509

combined fit to the number of observed events in all the final states. The likelihood is a combination of individual channel likelihoods for the signal and background hypotheses with the statistical and systematic uncertainties in the form of scaling nuisance parameters. The fiducial cross section is measured by scaling the cross section in the simulation by the ratio of the measured and predicted event yields given by the fit.

The definitions for the fiducial phase spaces for the $Z \to 4\ell$ and $ZZ \to 4\ell$ cross section measurements are given in Table 4. In the $ZZ \to 4\ell$ case, the Z bosons used in the fiducial definition are built by pairing final-state leptons using the same algorithm as is used to build Z boson candidates from reconstructed leptons. The generator-level leptons used for the fiducial cross section calculation are "dressed" by adding the momenta of generator-level photons within $\Delta R(\ell, \gamma) < 0.1$ to their momenta.

The measured cross sections are

$$\begin{aligned}&\sigma_{\text{fid}}(\text{pp} \to \text{Z} \to 4\ell)\\ &\quad = 31.2^{+1.5}_{-1.4}\,(\text{stat})^{+2.1}_{-1.9}\,(\text{syst}) \pm 0.8\,(\text{lumi})\ \text{fb},\\ &\sigma_{\text{fid}}(\text{pp} \to \text{ZZ} \to 4\ell)\\ &\quad = 40.9 \pm 1.3\,(\text{stat}) \pm 1.4\,(\text{syst}) \pm 1.0\,(\text{lumi})\ \text{fb}.\end{aligned} \tag{2}$$

The $\text{pp} \to \text{Z} \to 4\ell$ fiducial cross section can be compared to $27.9^{+1.0}_{-1.5} \pm 0.6$ fb calculated at NLO in QCD with POWHEG using the same settings as used for the simulated sample described in Sect. 3, with dynamic scales $\mu_{\text{F}} = \mu_{\text{R}} = m_{4\ell}$. The uncertainties correspond to scale and PDF variations, respectively. The ZZ fiducial cross section can be compared to $34.4^{+0.7}_{-0.6} \pm 0.5$ fb calculated with POWHEG and MCFM using the same settings as the simulated samples, or to $36.0^{+0.9}_{-0.8}$ computed with MATRIX at NNLO. The POWHEG and MATRIX calculations used dynamic scales $\mu_{\text{F}} = \mu_{\text{R}} = m_{4\ell}$, while the contribution from MCFM was computed with dynamic scales $\mu_{\text{F}} = \mu_{\text{R}} = 0.5 m_{4\ell}$.

The $\text{pp} \to \text{Z} \to 4\ell$ fiducial cross section is scaled to $\sigma(\text{pp} \to \text{Z})\mathcal{B}(\text{Z} \to 4\ell)$ using the acceptance correction factor $\mathcal{A} = 0.125 \pm 0.002$, estimated with POWHEG. This factor

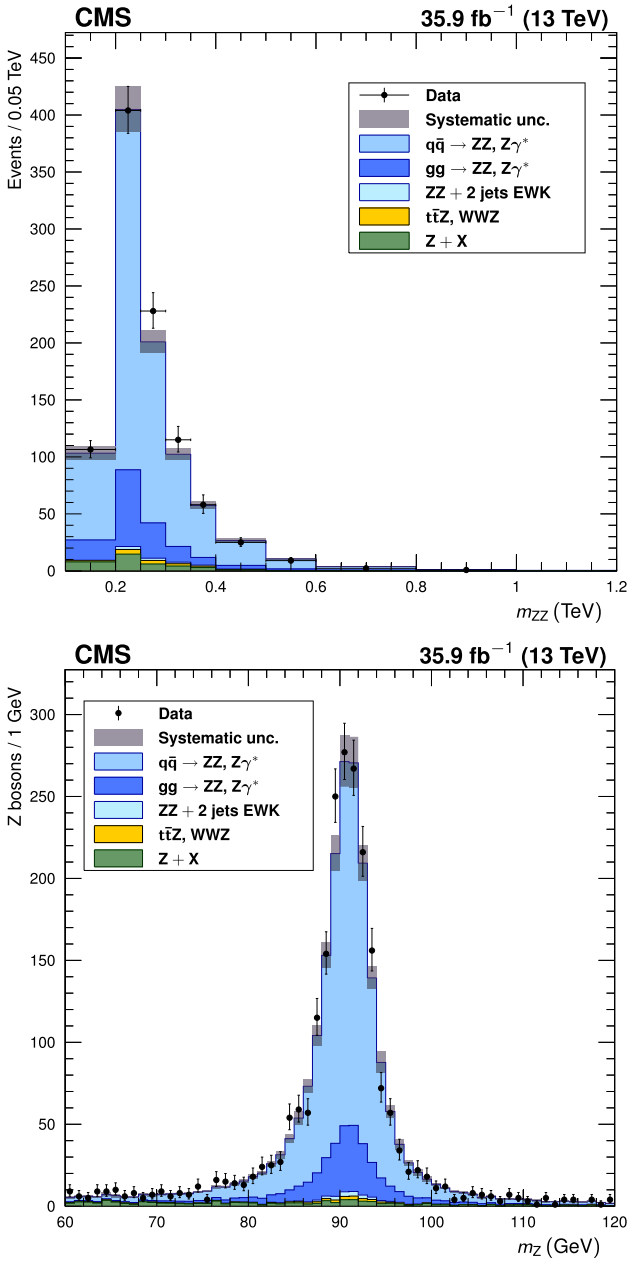

Fig. 4 Distributions of (upper) the four-lepton invariant mass m_{ZZ} and (lower) dilepton candidate mass for four-lepton events selected with both Z bosons on-shell. Points represent the data, while filled histograms represent the SM prediction and background estimate. Vertical bars on the data points show their statistical uncertainty. Shaded grey regions around the predicted yield represent combined statistical, systematic, theoretical, and integrated luminosity uncertainties. In the m_{ZZ} distribution, bin contents are normalized to the bin widths, using a unit bin size of 50 GeV; horizontal bars on the data points show the range of the corresponding bin

corrects the fiducial $Z \to 4\ell$ cross section to the phase space with only the 80–100 GeV mass window and $m_{\ell^+\ell^-} > 4$ GeV requirements, and also includes a correction, 0.96 ± 0.01, for the contribution of nonresonant four-lepton production to the

Table 3 The observed and expected yields of ZZ events, and estimated yields of background events, shown for each final state and summed in the total expected yield. The first uncertainty is statistical, the second one is systematic. The systematic uncertainties do not include the uncertainty in the integrated luminosity

Decay channel	Expected $N_{4\ell}$	Background	Total expected	Observed
4μ	$301 \pm 2 \pm 9$	$10 \pm 1 \pm 2$	$311 \pm 2 \pm 9$	335
2e2μ	$503 \pm 2 \pm 19$	$31 \pm 2 \pm 4$	$534 \pm 3 \pm 20$	543
4e	$205 \pm 1 \pm 12$	$20 \pm 2 \pm 2$	$225 \pm 2 \pm 13$	220
Total	$1009 \pm 3 \pm 36$	$60 \pm 3 \pm 8$	$1070 \pm 4 \pm 37$	1098

signal region. The uncertainty takes into account the interference between doubly- and singly-resonant diagrams. The measured cross section is

$$\sigma(\mathrm{pp} \to \mathrm{Z})\mathcal{B}(\mathrm{Z} \to 4\ell) = 249 \pm 11(stat)^{+16}_{-15}(syst) \pm 4(theo) \pm 6(lumi)\,fb \quad (3)$$

The branching fraction for the $\mathrm{Z} \to 4\ell$ decay, $\mathcal{B}(\mathrm{Z} \to 4\ell)$, is measured by comparing the cross section given by Eq. (3) with the $\mathrm{Z} \to \ell^+\ell^-$ cross section, and is computed as

$$\mathcal{B}(\mathrm{Z} \to 4\ell) = \frac{\sigma(\mathrm{pp} \to \mathrm{Z} \to 4\ell)}{\mathcal{C}^{60\text{–}120}_{80\text{–}100}\,\sigma(\mathrm{pp} \to \mathrm{Z} \to \ell^+\ell^-)/\mathcal{B}(\mathrm{Z} \to \ell^+\ell^-)}, \quad (4)$$

where $\sigma(\mathrm{pp} \to \mathrm{Z} \to \ell^+\ell^-) = 1870^{+50}_{-40}$ pb is the $\mathrm{Z} \to \ell^+\ell^-$ cross section times branching fraction calculated at NNLO with FEWZ v2.0 [50] in the mass range 60–120 GeV. Its uncertainty includes PDF uncertainties and uncertainties in α_s, the charm and bottom quark masses, and the effect of neglected higher-order corrections to the calculation. The factor $\mathcal{C}^{60\text{–}120}_{80\text{–}100} = 0.926 \pm 0.001$ corrects for the difference in Z boson mass windows and is estimated using POWHEG. Its uncertainty includes scale and PDF variations. The nominal Z to dilepton branching fraction $\mathcal{B}(\mathrm{Z} \to \ell^+\ell^-)$ is 0.03366 [46]. The measured value is

$$\mathcal{B}(\mathrm{Z} \to 4\ell) = 4.83^{+0.23}_{-0.22}(stat)^{+0.32}_{-0.29}(syst) \pm 0.08(theo) \pm 0.12(lumi) \times 10^{-6} \quad (5)$$

where the theoretical uncertainty includes the uncertainties in $\sigma(\mathrm{pp} \to \mathrm{Z})\mathcal{B}(\mathrm{Z} \to \ell^+\ell^-)$, $\mathcal{C}^{60\text{–}120}_{80\text{–}100}$, and $\mathcal{A}$. This can be compared with 4.6×10^{-6}, computed with MADGRAPH5_aMC@NLO, and is consistent with the CMS and ATLAS measurements at $\sqrt{s} = 7$, 8, and 13 TeV [6,14,15].

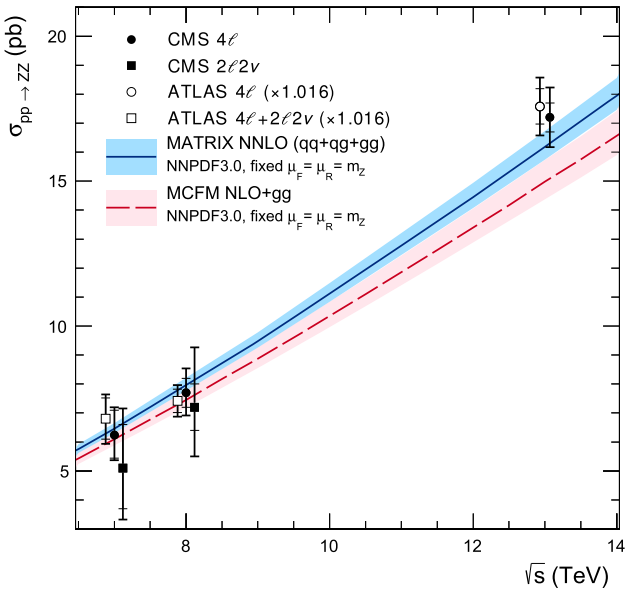

Fig. 5 The total ZZ cross section as a function of the proton-proton center-of-mass energy. Results from the CMS and ATLAS experiments are compared to predictions from MATRIX at NNLO in QCD, and MCFM at NLO in QCD. The MCFM prediction also includes gluon-gluon initiated production at LO in QCD. Both predictions use NNPDF3.0 PDF sets and fixed scales $\mu_\mathrm{F} = \mu_\mathrm{R} = m_\mathrm{Z}$. Details of the calculations and uncertainties are given in the text. The ATLAS measurements were performed with a Z boson mass window of 66–116 GeV, and are corrected for the resulting 1.6% difference. Measurements at the same center-of-mass energy are shifted slightly along the horizontal axis for clarity

The total ZZ production cross section for both dileptons produced in the mass range 60–120 GeV and $m_{\ell^+\ell'^-} > 4$ GeV is found to be

$$\sigma(\mathrm{pp} \to \mathrm{ZZ}) = 17.5^{+0.6}_{-0.5}\,(\mathrm{stat}) \pm 0.6\,(\mathrm{syst}) \pm 0.4\,(\mathrm{theo}) \pm 0.4\,(\mathrm{lumi})\ \mathrm{pb}. \quad (6)$$

The measured total cross section can be compared to the theoretical value of $14.5^{+0.5}_{-0.4} \pm 0.2$ pb calculated with a combination of POWHEG and MCFM with the same settings as described for $\sigma_\mathrm{fid}(\mathrm{pp} \to \mathrm{ZZ} \to 4\ell)$. It can also be compared to $16.2^{+0.6}_{-0.4}$ pb, calculated at NNLO in QCD via MATRIX v1.0.0_beta4 [11,51], or $15.0^{+0.7}_{-0.6} \pm 0.2$ pb, calculated with MCFM at NLO in QCD with additional contributions from LO gg $\to$ ZZ diagrams. Both values are calculated with the NNPDF3.0 PDF sets, at NNLO and NLO, respectively, and fixed scales set to $\mu_\mathrm{F} = \mu_\mathrm{R} = m_\mathrm{Z}$.

This measurement agrees with the previously published cross section measured by CMS at 13 TeV [6] based on a 2.6 fb^{-1} data sample collected in 2015:

$$\sigma(\mathrm{pp} \to \mathrm{ZZ}) = 14.6^{+1.9}_{-1.8}\,(\mathrm{stat})^{+0.3}_{-0.5}\,(\mathrm{syst}) \pm 0.2\,(\mathrm{theo}) \pm 0.4\,(\mathrm{lumi})\ \mathrm{pb}. \quad (7)$$

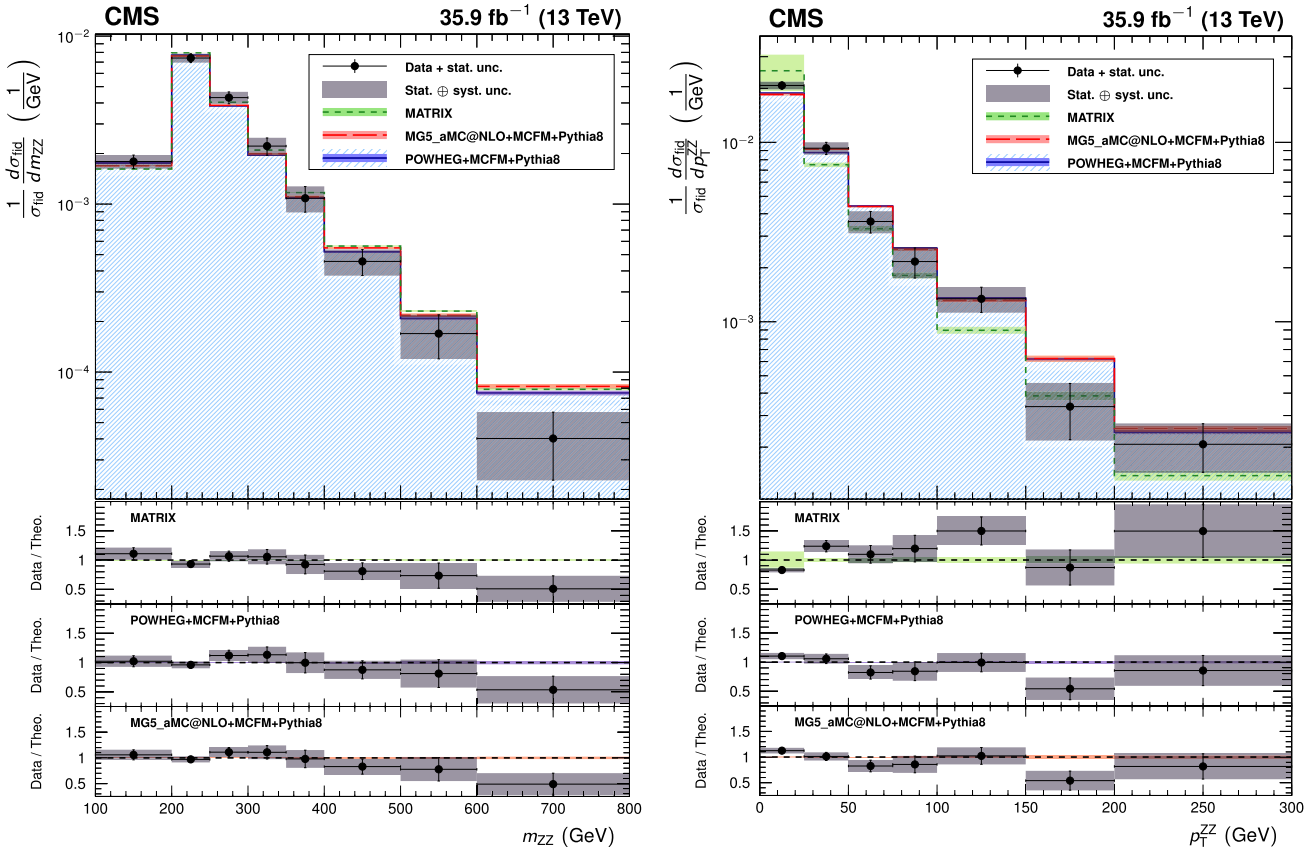

Fig. 6 Differential cross sections normalized to the fiducial cross section for the combined 4e, 4μ, and 2e2μ decay channels as a function of mass (left) and p_T (right) of the ZZ system. Points represent the unfolded data; the solid, dashed, and dotted histograms represent the POWHEG+MCFM, MADGRAPH5_aMC@NLO+MCFM, and MATRIX predictions for ZZ signal, respectively, and the bands around the predictions reflect their combined statistical, scale, and PDF uncertainties PYTHIA v8 was used for parton showering, hadronization, and underlying event simulation in the POWHEG, MADGRAPH5_aMC@NLO, and MCFM samples. The lower part of each plot represents the ratio of the measured cross section to the theoretical distributions. The shaded grey areas around the points represent the sum in quadrature of the statistical and systematic uncertainties, while the crosses represent the statistical uncertainties only

The two measurements can be combined to yield the "2015 + 2016 cross section"

$$\sigma(\mathrm{pp} \to \mathrm{ZZ}) = 17.2 \pm 0.5\,(\mathrm{stat}) \pm 0.7\,(\mathrm{syst}) \pm 0.4\,(\mathrm{theo}) \pm 0.4\,(\mathrm{lumi})\ \mathrm{pb}. \quad (8)$$

The combination was performed once considering the experimental uncertainties to be fully correlated between the 2015 and 2016 data sets, and once considering them to be fully uncorrelated. The results were averaged, and the difference was added linearly to the systematic uncertainty in the combined cross section.

The total ZZ cross section is shown in Fig. 5 as a function of the proton-proton center-of-mass energy. Results from CMS [3,4] and ATLAS [7,8,10] are compared to predictions from MATRIX and MCFM with the NNPDF3.0 PDF sets and fixed scales $\mu_F = \mu_R = m_Z$. The MATRIX prediction uses PDFs calculated at NNLO, while the MCFM prediction uses NLO PDFs. The uncertainties are statistical (inner bars) and statistical and systematic added in quadrature (outer bars). The band around the MATRIX predictions reflects scale uncertainties, while the band around the MCFM predictions reflects both scale and PDF uncertainties.

The measurement of the differential cross sections provides detailed information about ZZ kinematics. The observed yields are unfolded using the iterative technique described in Ref. [52]. Unfolding is performed with the RooUnfold package [53] and regularized by stopping after four iterations. Statistical uncertainties in the data distributions are propagated through the unfolding process to give the statistical uncertainties on the normalized differential cross sections.

The three decay channels, 4e, 4μ, and 2e2μ, are combined after unfolding because no differences are expected in their kinematic distributions. The generator-level leptons used for the unfolding are dressed as in the fiducial cross section calculation.

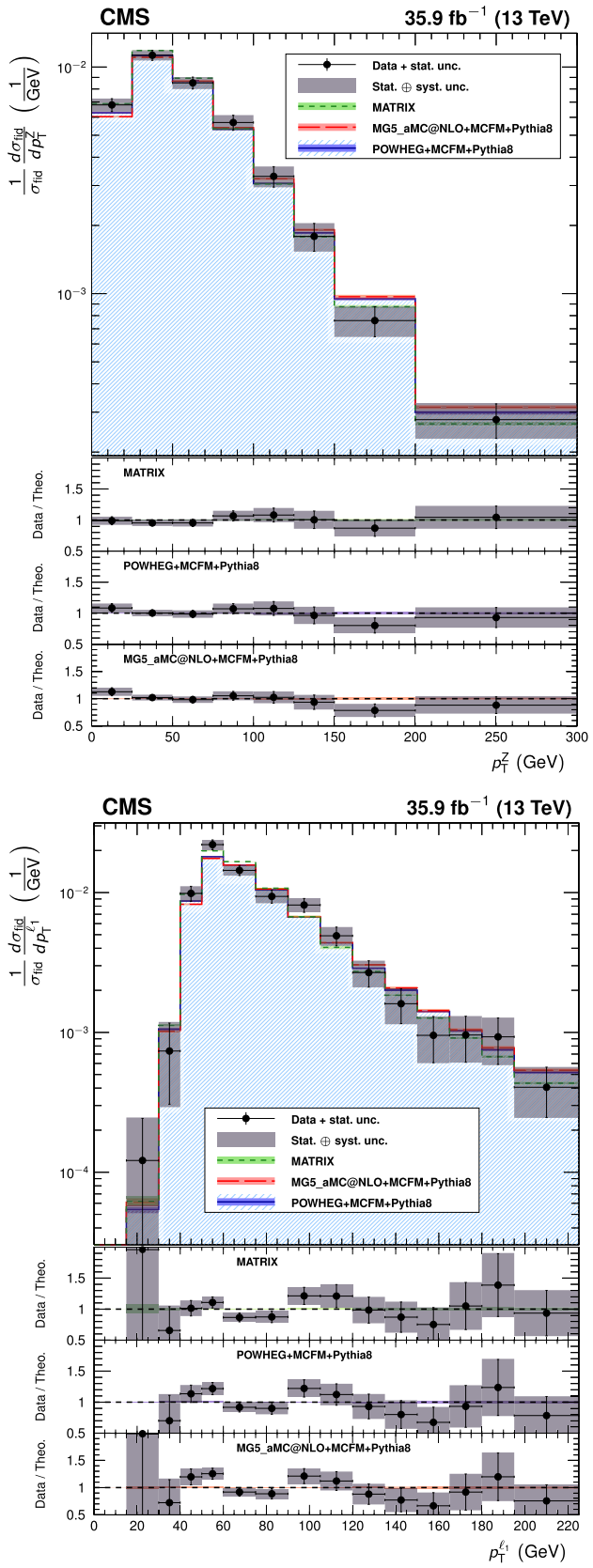

Fig. 7 Normalized ZZ differential cross sections as a function of the p_T of (upper) all Z bosons and (lower) the leading lepton in ZZ events. Other details are as described in the caption of Fig. 6

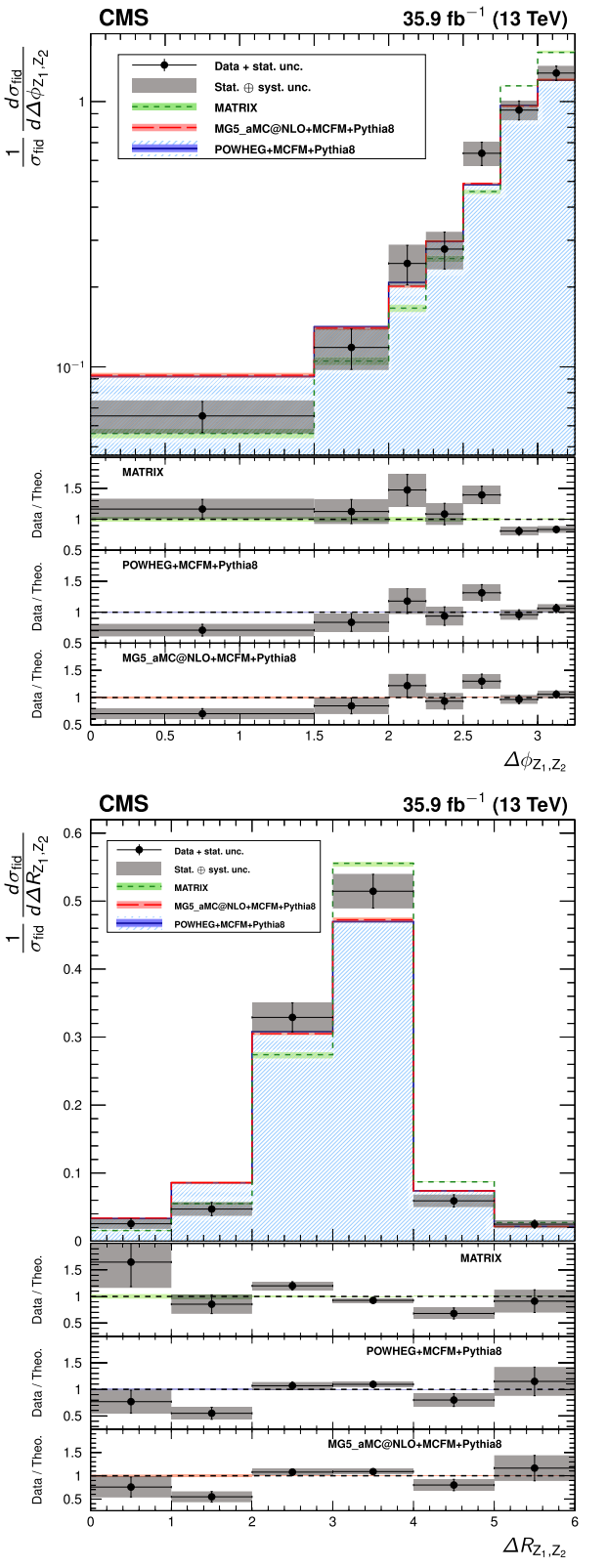

Fig. 8 Normalized ZZ differential cross sections as a function of (upper) the azimuthal separation of the two Z bosons and (lower) ΔR between the Z-bosons. Other details are as described in the caption of Fig. 6

Table 4 Fiducial definitions for the reported cross sections. The common requirements are applied for both measurements

Cross section measurement	Fiducial requirements
Common requirements	$p_{\mathrm{T}}^{\ell_1} > 20\,\mathrm{GeV}$, $p_{\mathrm{T}}^{\ell_2} > 10\,\mathrm{GeV}$, $p_{\mathrm{T}}^{\ell_{3,4}} > 5\,\mathrm{GeV}$, $\lvert\eta^{\ell}\rvert < 2.5$, $m_{\ell\ell} > 4\,\mathrm{GeV}$ (any opposite-sign same-flavor pair)
$\mathrm{Z} \to 4\ell$	$m_{\mathrm{Z}_1} > 40\,\mathrm{GeV}$
	$80 < m_{4\ell} < 100\,\mathrm{GeV}$
$\mathrm{ZZ} \to 4\ell$	$60 < (m_{\mathrm{Z}_1}, m_{\mathrm{Z}_2}) < 120\,\mathrm{GeV}$

The differential distributions normalized to the fiducial cross sections are presented in Figs. 6, 7, 8 for the combination of the 4e, 4μ, and 2e2μ decay channels. The fiducial cross section definition includes p_{T}^{ℓ} and $|\eta^{\ell}|$ selections on each lepton, and the 60–120 GeV mass requirement, as described in Table 4 and Sect. 4. Figure 6 shows the normalized differential cross sections as functions of the mass and p_{T} of the ZZ system, Fig. 7 shows them as functions of the p_{T} of all Z bosons and the p_{T} of the leading lepton in each event, and Fig. 8 shows the angular correlations between the two Z bosons. The data are corrected for background contributions and compared with the theoretical predictions from POWHEG and MCFM, MADGRAPH5_aMC@NLO and MCFM, and MATRIX. The bottom part of each plot shows the ratio of the measured to the predicted values. The bin sizes are chosen according to the resolution of the relevant variables, while also keeping the statistical uncertainties at a similar level in all bins. The data are well reproduced by the simulation except in the low p_{T} regions, where data tend to have a steeper slope than the prediction.

Figure 9 shows the normalized differential four-lepton cross section as a function of $m_{4\ell}$, subject only to the common requirements of Table 4. This includes contributions from the Z and Higgs boson resonances and continuum ZZ production.

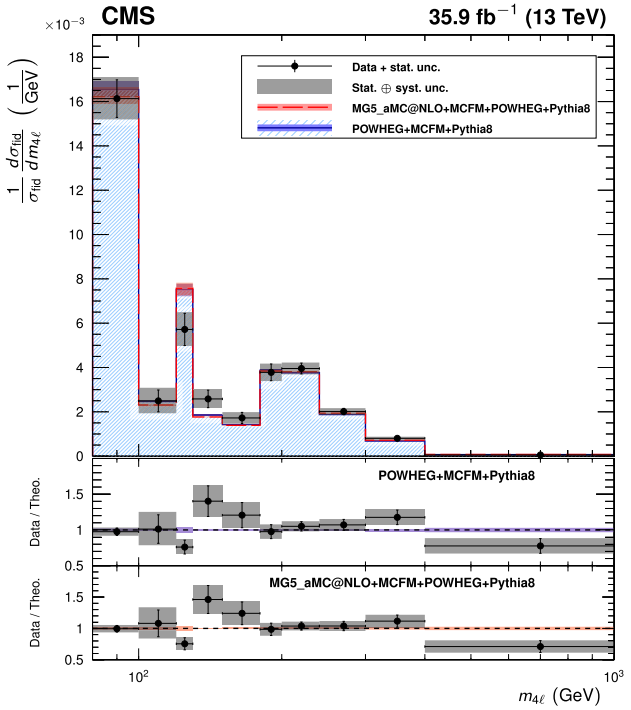

Fig. 9 The normalized differential four-lepton cross section as a function of the four-lepton mass, subject only to the common requirements of Table 4. SM $\mathrm{gg} \to \mathrm{H} \to \mathrm{ZZ}^*$ production is included, simulated with POWHEG. Other details are as described in the caption of Fig. 6

9 Limits on anomalous triple gauge couplings

The presence of aTGCs would increase the yield of events at high four-lepton masses. Figure 10 presents the distribution of the four-lepton reconstructed mass of events with both Z bosons in the mass range 60–120 GeV for the combined 4e, 4μ, and 2e2μ channels. This distribution is used to set the limits on possible contributions from aTGCs. Two simulated samples with nonzero aTGCs are shown as examples, along with the SM distribution simulated by both SHERPA and POWHEG.

The invariant mass distributions are interpolated from the SHERPA simulations for different values of the anomalous couplings in the range between 0 and 0.015. For each distribution, only one or two couplings are varied while all others are set to zero. The measured signal is obtained from a comparison of the data to a grid of aTGC models in the $(f_4^{\mathrm{Z}}, f_4^{\gamma})$ and $(f_5^{\mathrm{Z}}, f_5^{\gamma})$ parameter planes. Expected signal values are interpolated between the 2D grid points using a second-degree polynomial, since the cross section for the signal depends quadratically on the coupling parameters. A binned profile likelihood method, Wald Gaussian approximation, and Wilk's theorem are used to derive one-dimensional limits at a 95% confidence level (CL) on each of the four aTGC parameters, and two-dimensional limits at a 95% CL on the pairs $(f_4^{\mathrm{Z}}, f_4^{\gamma})$ and $(f_5^{\mathrm{Z}}, f_5^{\gamma})$ [46,54,55]. When the limits are calculated for each parameter or pair, all other parameters are set to their SM values. The systematic uncertainties described in Sect. 7 are treated as nuisance parameters with log-normal distributions. No form factor is used when deriving the limits so that the results do not depend on any assumed energy scale characterizing new physics. The constraints on anomalous couplings are displayed in Fig. 11. The curves indicate 68 and 95% confidence levels, and the solid dot shows the coordinates where the likelihood reaches its maximum. Coupling values outside the contours are excluded at

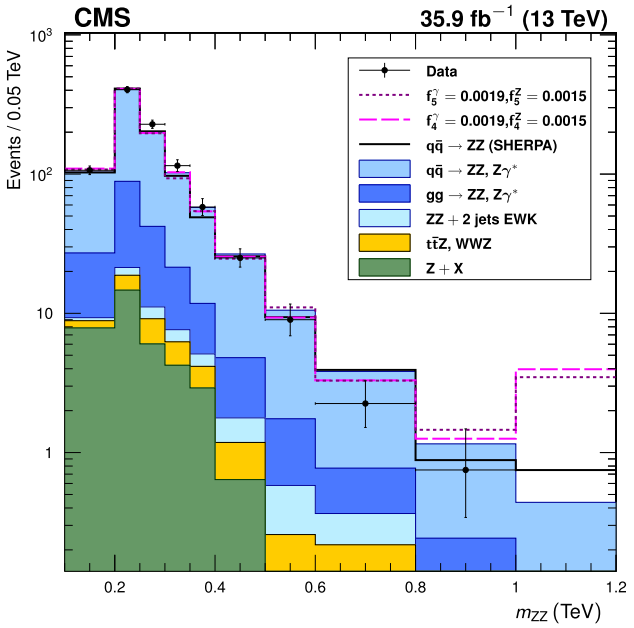

Fig. 10 Distribution of the four-lepton reconstructed mass for the combined 4e, 4μ, and 2e2μ channels. Points represent the data, the filled histograms represent the SM expected yield including signal and irreducible background predictions from simulation and the data-driven background estimate. Unfilled histograms represent examples of aTGC signal predictions (dashed), and the SHERPA SM prediction (solid), included to illustrate the expected shape differences between the SHERPA and POWHEG predictions. Vertical bars on the data points show their statistical uncertainty. The SHERPA distributions are normalized such that the SM sample has the same total yield as the POWHEG sample predicts. Bin contents are normalized to the bin widths, using a unit bin size of 50 GeV; horizontal bars on the data points show the range of the corresponding bin. The last bin includes the "overflow" contribution from events at masses above 1.2 TeV

the corresponding confidence levels. The limits are dominated by statistical uncertainties.

The observed one-dimensional 95% CL limits for the $f_4^{Z,\gamma}$ and $f_5^{Z,\gamma}$ anomalous coupling parameters are:

$$\begin{aligned} -0.0012 < f_4^Z < 0.0010, \quad -0.0010 < f_5^Z < 0.0013, \\ -0.0012 < f_4^\gamma < 0.0013, \quad -0.0012 < f_5^\gamma < 0.0013. \end{aligned} \tag{9}$$

These are the most stringent limits to date on anomalous ZZZ and ZZγ trilinear gauge boson couplings, improving on the previous strictest results from CMS [5] by factors of two or more and constraining the coupling parameters more than the corresponding ATLAS results [10].

One way to impose unitarity on the aTGC models is to restrict the range of four-lepton invariant mass used in the limit calculation. The limits will then depend on the "cutoff" value used. The computation of the one-dimensional limits is repeated for different maximum allowed values of $m_{4\ell}$, and the results are presented in Fig. 12 as a function of this cutoff.

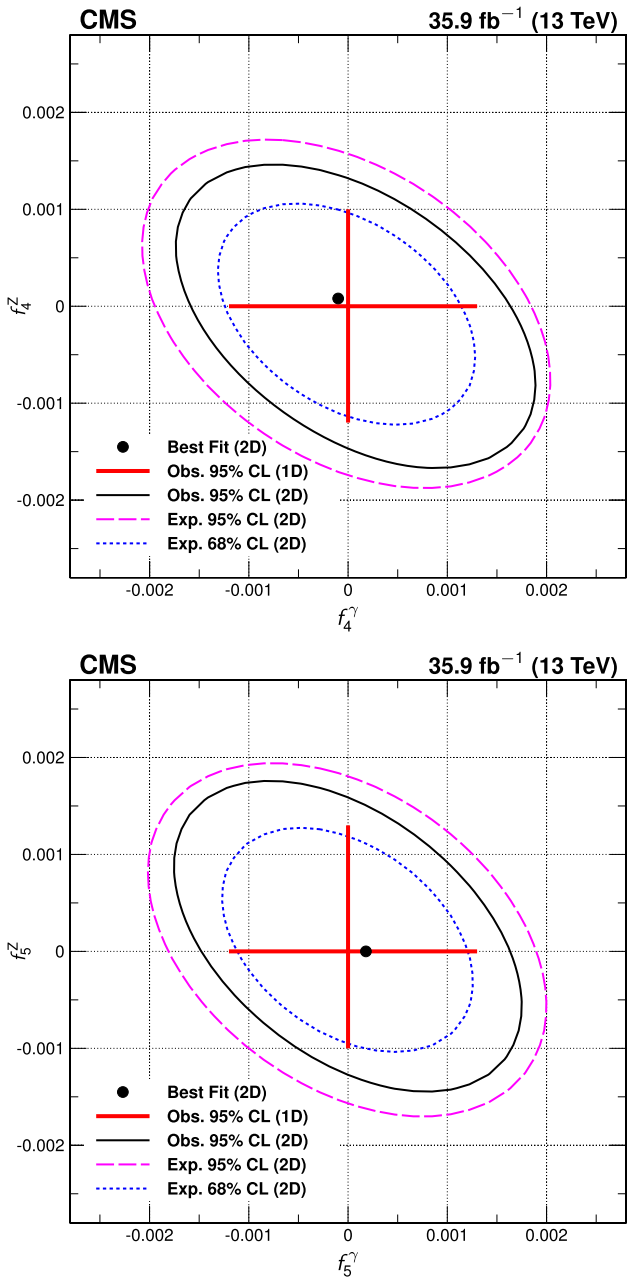

Fig. 11 Two-dimensional observed 95% CL limits (solid contour) and expected 68 and 95% CL limits (dashed contour) on the ZZZ and ZZγ aTGCs. The upper(lower) plot shows the exclusion contour in the $f_{4(5)}^Z$, $f_{4(5)}^\gamma$ parameter planes. The values of couplings outside of contours are excluded at the corresponding confidence level. The solid dot is the point at which the likelihood is at its maximum. The solid lines at the center show the observed one-dimensional 95% CL limits for $f_{4,5}^\gamma$ (horizontal) and $f_{4,5}^Z$ (vertical). No form factor is used

10 Summary

A series of measurements of four-lepton final states in proton-proton collisions at $\sqrt{s} = 13$ TeV have been performed with the CMS detector at the CERN LHC. The measured

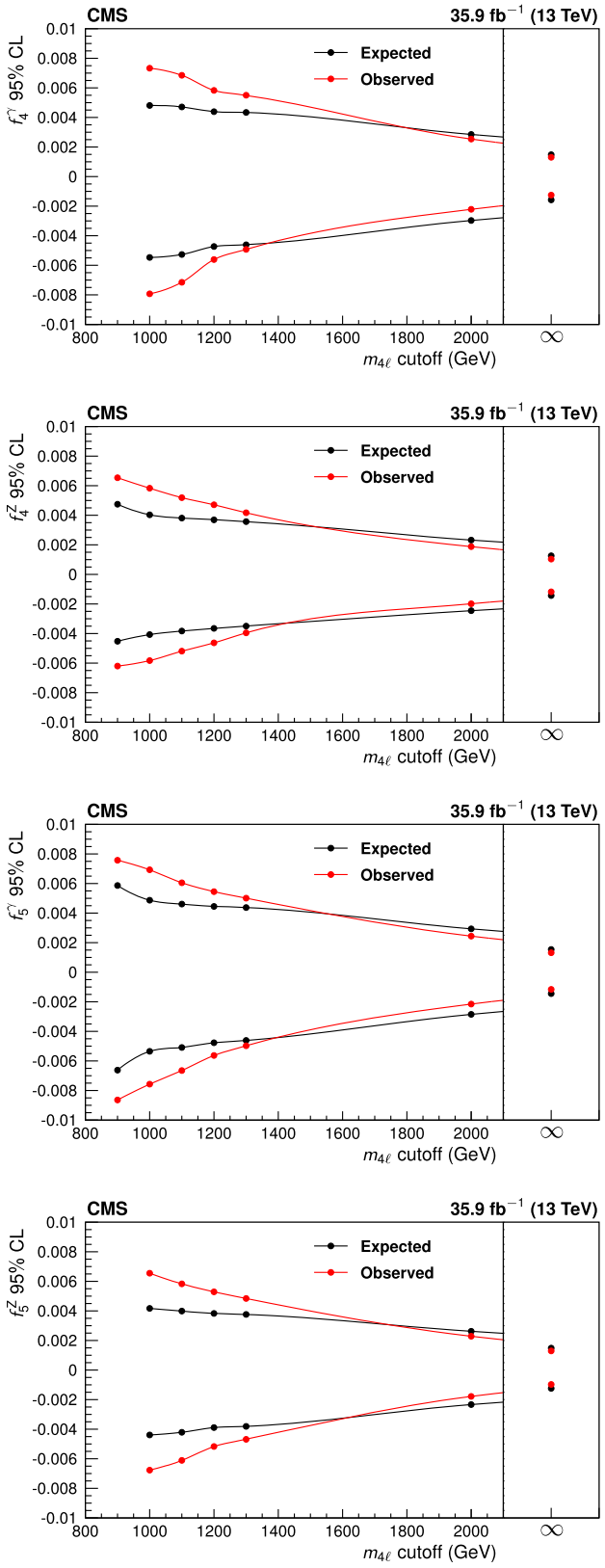

Fig. 12 Expected and observed one-dimensional limits on the four aTGC parameters, as a function of an upper cutoff on the invariant mass of the four-lepton system. No form factor is used

pp $\rightarrow$ ZZ cross section is $\sigma(\mathrm{pp} \rightarrow \mathrm{ZZ}) = 17.2 \pm 0.5\,(\mathrm{stat}) \pm 0.7\,(\mathrm{syst}) \pm 0.4\,(\mathrm{theo}) \pm 0.4\,(\mathrm{lumi})$ pb for Z boson masses in the range $60 < m_Z < 120$ GeV. The measured branching fraction for Z boson decays to four leptons is $\mathcal{B}(\mathrm{Z} \rightarrow 4\ell) = 4.83^{+0.23}_{-0.22}(stat)^{+0.32}_{-0.29}(syst) \pm 0.08(theo) \pm 0.12(lumi) \times 10^{-6}$ for four-lepton mass in the range $80 < m_{4\ell} < 100$ GeV and dilepton mass $m_{\ell\ell} > 4$ GeV for all oppositely charged same-flavor lepton pairs. Normalized differential cross sections were also measured. All results agree well with the SM predictions. Improved limits on anomalous ZZZ and ZZγ triple gauge couplings were established, the most stringent to date.

Acknowledgements We congratulate our colleagues in the CERN accelerator departments for the excellent performance of the LHC and thank the technical and administrative staffs at CERN and at other CMS institutes for their contributions to the success of the CMS effort. In addition, we gratefully acknowledge the computing centers and personnel of the Worldwide LHC Computing Grid for delivering so effectively the computing infrastructure essential to our analyses. Finally, we acknowledge the enduring support for the construction and operation of the LHC and the CMS detector provided by the following funding agencies: BMWFW and FWF (Austria); FNRS and FWO (Belgium); CNPq, CAPES, FAPERJ, and FAPESP (Brazil); MES (Bulgaria); CERN; CAS, MoST, and NSFC (China); COLCIENCIAS (Colombia); MSES and CSF (Croatia); RPF (Cyprus); SENESCYT (Ecuador); MoER, ERC IUT, and ERDF (Estonia); Academy of Finland, MEC, and HIP (Finland); CEA and CNRS/IN2P3 (France); BMBF, DFG, and HGF (Germany); GSRT (Greece); OTKA and NIH (Hungary); DAE and DST (India); IPM (Iran); SFI (Ireland); INFN (Italy); MSIP and NRF (Republic of Korea); LAS (Lithuania); MOE and UM (Malaysia); BUAP, CINVESTAV, CONACYT, LNS, SEP, and UASLP-FAI (Mexico); MBIE (New Zealand); PAEC (Pakistan); MSHE and NSC (Poland); FCT (Portugal); JINR (Dubna); MON, RosAtom, RAS, RFBR and RAEP (Russia); MESTD (Serbia); SEIDI, CPAN, PCTI and FEDER (Spain); Swiss Funding Agencies (Switzerland); MST (Taipei); ThEPCenter, IPST, STAR, and NSTDA (Thailand); TUBITAK and TAEK (Turkey); NASU and SFFR (Ukraine); STFC (United Kingdom); DOE and NSF (USA). Individuals have received support from the Marie-Curie program and the European Research Council and Horizon 2020 Grant, contract No. 675440 (European Union); the Leventis Foundation; the A. P. Sloan Foundation; the Alexander von Humboldt Foundation; the Belgian Federal Science Policy Office; the Fonds pour la Formation à la Recherche dans l'Industrie et dans l'Agriculture (FRIA-Belgium); the Agentschap voor Innovatie door Wetenschap en Technologie (IWT-Belgium); the Ministry of Education, Youth and Sports (MEYS) of the Czech Republic; the Council of Science and Industrial Research, India; the HOMING PLUS program of the Foundation for Polish Science, cofinanced from European Union, Regional Development Fund, the Mobility Plus program of the Ministry of Science and Higher Education, the National Science Center (Poland), contracts Harmonia 2014/14/M/ST2/00428, Opus 2014/13/B/ST2/02543, 2014/15/B/ST2/03998, and 2015/19/B/ST2/02861, Sonata-bis 2012/07/E/ST2/01406; the National Priorities Research Program by Qatar National Research Fund; the Programa Severo Ochoa del Principado de Asturias; the Thalis and Aristeia programs cofinanced by EU-ESF and the Greek NSRF; the Rachadapisek Sompot Fund for Postdoctoral Fellowship, Chulalongkorn University and the Chulalongkorn Academic into Its 2nd Century Project Advancement Project (Thailand); the Welch Foundation, contract C-1845; and the Weston Havens Foundation (USA).

Funded by SCOAP[3].

References

1. G.J. Gounaris, J. Layssac, F.M. Renard, New and standard physics contributions to anomalous Z and γ self-couplings. Phys. Rev. D **62**, 073013 (2000). https://doi.org/10.1103/PhysRevD.62.073013. arXiv:hep-ph/0003143
2. K. Hagiwara, R.D. Peccei, D. Zeppenfeld, Probing the weak boson sector in $e^+e^- \to W^+W^-$. Nucl. Phys. B **282**, 253 (1987). https://doi.org/10.1016/0550-3213(87)90685-7
3. CMS Collaboration, Measurement of the ZZ production cross section and search for anomalous couplings in $2\ell 2\ell'$ final states in pp collisions at $\sqrt{s} = 7$TeV, *JHEP***01**, 063 (2013). https://doi.org/10.1007/JHEP01(2013)063. arXiv:1211.4890
4. CMS Collaboration, Measurement of the pp $\to$ ZZ production cross section and constraints on anomalous triple gauge couplings in four-lepton final states at $\sqrt{s} = 8$TeV, Phys. Lett. B **740**, 250 (2015). https://doi.org/10.1016/j.physletb.2014.11.059. arXiv:1406.0113. Corrigenum: https://doi.org/10.1016/j.physletb.2016.04.010
5. CMS Collaboration, Measurements of the ZZ production cross sections in the $2\ell 2\nu$ channel in proton-proton collisions at $\sqrt{s} = 7$ and 8TeV and combined constraints on triple gauge couplings, Eur. Phys. J. C. **75**, 511 (2015). https://doi.org/10.1140/epjc/s10052-015-3706-0. arXiv:1503.05467
6. CMS Collaboration, Measurement of the ZZ production cross section and Z $\to \ell^+\ell^-\ell'^+\ell'^-$ branching fraction in pp collisions at $\sqrt{s} = 13$TeV. Phys. Lett. B **763**, 280 (2016). https://doi.org/10.1016/j.physletb.2016.10.054. arXiv:1607.08834
7. ATLAS Collaboration, Measurement of ZZ production in pp collisions at $\sqrt{s} = 7$TeV and limits on anomalous ZZZ and ZZγ couplings with the ATLAS detector. JHEP **03**, 128 (2013). https://doi.org/10.1007/JHEP03(2013)128. arXiv:1211.6096
8. ATLAS Collaboration, Measurements of four-lepton production in pp collisions at $\sqrt{s} = 8$TeV with the ATLAS detector. Phys. Lett. B. **753**, 552 (2016). https://doi.org/10.1016/j.physletb.2015.12.048. arXiv:1509.07844
9. ATLAS Collaboration, Measurement of the ZZ production cross section in pp collisions at $\sqrt{s} = 13$TeV with the ATLAS detector. Phys. Rev. Lett. **116**, 101801 (2016). https://doi.org/10.1103/PhysRevLett.116.101801. arXiv:1512.05314
10. ATLAS Collaboration, ZZ $\to \ell^+\ell^-\ell'^+\ell'^-$ cross-section measurements and search for anomalous triple gauge couplings in 13 TeV pp collisions with the ATLAS detector. Phys. Rev. D 97, 032005 (2018). https://doi.org/10.1103/PhysRevD.97.032005. arXiv:1709.07703
11. F. Cascioli et al., ZZ production at hadron colliders in NNLO QCD. Phys. Lett. B **735**, 311 (2014). https://doi.org/10.1016/j.physletb.2014.06.056. arXiv:1405.2219
12. ATLAS Collaboration, Measurement of the ZZ production cross section in proton-proton collisions at $\sqrt{s} = 8$TeV using the ZZ $\to \ell^-\ell^+\ell'^-\ell'^+$ and ZZ $\to \ell^-\ell^+\nu\bar{\nu}$ channels with the ATLAS detector. JHEP **01**, 099 (2017). https://doi.org/10.1007/JHEP01(2017)099. arXiv:1610.07585
13. ALEPH Collaboration, Study of the four fermion final state at the Z resonance. Z. Phys. C. **66**, 3 (1995). https://doi.org/10.1007/BF01496576
14. CMS Collaboration, Observation of Z decays to four leptons with the CMS detector at the LHC. JHEP. **12**, 034 (2012). https://doi.org/10.1007/JHEP12(2012)034. arXiv:1210.3844
15. ATLAS Collaboration, Measurements of four-lepton production at the Z resonance in pp collisions at $\sqrt{s} = 7$ and 8TeV with ATLAS. Phys. Rev. Lett. 112, 231806 (2014). https://doi.org/10.1103/PhysRevLett.112.231806. arXiv:1403.5657
16. CMS Collaboration, Measurements of properties of the Higgs boson decaying into the four-lepton final state in pp collisions at $\sqrt{s} = 13$TeV. JHEP 11, 047 (2017). https://doi.org/10.1007/JHEP11(2017)047. arXiv:1706.09936
17. CMS Collaboration, The CMS experiment at the CERN LHC, *JINST* **3**, S08004 (2008). https://doi.org/10.1088/1748-0221/3/08/S08004
18. CMS Collaboration, Performance of electron reconstruction and selection with the CMS detector in proton-proton collisions at $\sqrt{s} = 8$TeV, JINST. **10**, P06005 (2015). https://doi.org/10.1088/1748-0221/10/06/P06005. arXiv:1502.02701
19. CMS Collaboration, Performance of CMS muon reconstruction in pp collision events at $\sqrt{s} = 7$TeV. JINST, **7**, P10002 (2012). https://doi.org/10.1088/1748-0221/7/10/P10002. arXiv:1206.4071
20. S. Alioli, P. Nason, C. Oleari, E. Re, NLO vector-boson production matched with shower in POWHEG. JHEP **07**, 060 (2008). https://doi.org/10.1088/1126-6708/2008/07/060. arXiv:0805.4802
21. P. Nason, A new method for combining NLO QCD with shower Monte Carlo algorithms. JHEP **11**, 040 (2004). https://doi.org/10.1088/1126-6708/2004/11/040. arXiv:hep-ph/0409146
22. S. Frixione, P. Nason, C. Oleari, Matching NLO QCD computations with parton shower simulations: the POWHEG method. JHEP **11**, 070 (2007). https://doi.org/10.1088/1126-6708/2007/11/070. arXiv:0709.2092
23. S. Alioli, P. Nason, C. Oleari, E. Re, A general framework for implementing NLO calculations in shower Monte Carlo programs: the POWHEG BOX. JHEP **06**, 043 (2010). https://doi.org/10.1007/JHEP06(2010)043. arXiv:1002.2581
24. T. Melia, P. Nason, R. Rontsch, G. Zanderighi, W^+W^-, WZ and ZZ production in the POWHEG BOX. JHEP **11**, 078 (2011). https://doi.org/10.1007/JHEP11(2011)078. arXiv:1107.5051
25. J.M. Campbell, R.K. Ellis, MCFM for the Tevatron and the LHC. Nucl. Phys. B Proc. Suppl. **10**, 205 (2010). https://doi.org/10.1016/j.nuclphysbps.2010.08.011. arXiv:1007.3492
26. F. Caola, K. Melnikov, R. Röntsch, L. Tancredi, QCD corrections to ZZ production in gluon fusion at the LHC. Phys. Rev. D **92**, 094028 (2015). https://doi.org/10.1103/PhysRevD.92.094028. arXiv:1509.06734
27. A. Ballestrero et al., PHANTOM: A Monte Carlo event generator for six parton final states at high energy colliders. Comput. Phys. Commun. **180**, 401 (2009). https://doi.org/10.1016/j.cpc.2008.10.005. arXiv:0801.3359
28. Y. Gao et al., Spin determination of single-produced resonances at hadron colliders. Phys. Rev. D **81**, 075022 (2010). https://doi.org/10.1103/PhysRevD.81.075022. arXiv:1001.3396
29. S. Bolognesi et al., Spin and parity of a single-produced resonance at the LHC. Phys. Rev. D **86**, 095031 (2012). https://doi.org/10.1103/PhysRevD.86.095031. arXiv:1208.4018
30. I. Anderson et al., Constraining anomalous HVV interactions at proton and lepton colliders. Phys. Rev. D **89**, 035007 (2014). https://doi.org/10.1103/PhysRevD.89.035007. arXiv:1309.4819
31. J. Alwall et al., The automated computation of tree-level and next-to-leading order differential cross sections, and their matching to parton shower simulations. JHEP **07**, 079 (2014). https://doi.org/10.1007/JHEP07(2014)079. arXiv:1405.0301
32. T. Gleisberg et al., Event generation with SHERPA 1.1. JHEP **02**, 007 (2009). https://doi.org/10.1088/1126-6708/2009/02/007. arXiv:0811.4622

33. T. Sjöstrand, S. Mrenna, P. Skands, PYTHIA 6.4 physics and manual. JHEP **05**, 026 (2006). https://doi.org/10.1088/1126-6708/2006/05/026. arXiv:hep-ph/0603175
34. T. Sjöstrand et al., An introduction to PYTHIA 8.2. Comput. Phys. Commun. **191**, 159 (2015). https://doi.org/10.1016/j.cpc.2015.01.024. arXiv:1410.3012
35. CMS Collaboration, Event generator tunes obtained from underlying event and multiparton scattering measurements, *Eur. Phys. J. C* **76**, 155 (2016). https://doi.org/10.1140/epjc/s10052-016-3988-x. arXiv:1512.00815
36. NNPDF Collaboration, Parton distributions for the LHC run II. JHEP, **04**, 040 (2015). https://doi.org/10.1007/JHEP04(2015)040. arXiv:1410.8849
37. GEANT4 Collaboration, GEANT4–a simulation toolkit. Nucl. Instrum. Meth. A **506**, 250 (2003). https://doi.org/10.1016/S0168-9002(03)01368-8
38. CMS Collaboration, Particle-flow reconstruction and global event description with the CMS detector. JINST. **12**, P10003 (2017). https://doi.org/10.1088/1748-0221/12/10/P10003. arXiv:1706.04965
39. M. Cacciari, G.P. Salam, G. Soyez, The Anti-k_t jet clustering algorithm. JHEP **04**, 063 (2008). https://doi.org/10.1088/1126-6708/2008/04/063. arXiv:0802.1189
40. M. Cacciari, G.P. Salam, G. Soyez, FastJet user manual. Eur. Phys. J. C **72**, 1896 (2012). https://doi.org/10.1140/epjc/s10052-012-1896-2. arXiv:1111.6097
41. CMS Collaboration, Technical proposal for the phase-II upgrade of the Compact Muon Solenoid, CMS Technical proposal CERN-LHCC-2015-010, CMS-TDR-15-02, CERN, 2015. https://cds.cern.ch/record/2020886
42. M. Cacciari, G.P. Salam, Pileup subtraction using jet areas. Phys. Lett. B **659**, 119 (2008). https://doi.org/10.1016/j.physletb.2007.09.077. arXiv:0707.1378
43. CMS Collaboration, Measurement of the inclusive W and Z production cross sections in pp collisions at $\sqrt{s} = 7$TeV. JHEP, **10**, 132 (2011). https://doi.org/10.1007/JHEP10(2011)132. arXiv:1107.4789
44. CMS Collaboration, The CMS trigger system. JINST **12**, P01020 (2017). https://doi.org/10.1088/1748-0221/12/01/P01020. arXiv:1609.02366
45. CMS Collaboration, Measurement of the properties of a Higgs boson in the four-lepton final state. Phys. Rev. D **89**, 092007 (2014). https://doi.org/10.1103/PhysRevD.89.092007. arXiv:1312.5353
46. Particle Data Group, C. Patrignani et al., Review of particle physics. Chin. Phys C **40**, 100001 (2016). https://doi.org/10.1088/1674-1137/40/10/100001
47. J. Butterworth et al., PDF4LHC recommendations for LHC Run II. J. Phys. G **43**, 023001 (2016). https://doi.org/10.1088/0954-3899/43/2/023001. arXiv:1510.03865
48. CMS Collaboration, CMS luminosity measurements for the 2016 data taking period, CMS Physics Analysis Summary CMS-PAS-LUM-17-001, CERN, 2017. https://cds.cern.ch/record/2257069
49. ATLAS and CMS Collaborations, Combined measurement of the Higgs boson mass in pp collisions at $\sqrt{s} = 7$ and 8TeV with the ATLAS and CMS experiments. Phys. Rev. Lett. **114**, 191803 (2015). https://doi.org/10.1103/PhysRevLett.114.191803. arXiv:1503.07589
50. R. Gavin, Y. Li, F. Petriello, S. Quackenbush, FEWZ 2.0: A code for hadronic Z production at next-to-next-to-leading order. Comput. Phys. Commun. **182**, 2388 (2011). https://doi.org/10.1016/j.cpc.2011.06.008. arXiv:1011.3540
51. M. Grazzini, S. Kallweit, D. Rathlev, ZZ production at the LHC: fiducial cross sections and distributions in NNLO QCD. Phys. Lett. B **750**, 407 (2015). https://doi.org/10.1016/j.physletb.2015.09.055. arXiv:1507.06257
52. G. D'Agostini, A multidimensional unfolding method based on Bayes' theorem. Nucl. Instrum. Meth. A **362**, 487 (1995). https://doi.org/10.1016/0168-9002(95)00274-X
53. T. Adye, Unfolding algorithms and tests using RooUnfold, in *Proceedings, PHYSTAT 2011 Workshop on Statistical Issues Related to Discovery Claims in Search Experiments and Unfolding*, H. Prosper and L. Lyons, eds., p. 313, CERN. Geneva, Switzerland, 17–20 January, 2011. https://doi.org/10.5170/CERN-2011-006.313. arXiv:1105.1160
54. S.S. Wilks, The large-sample distribution of the likelihood ratio for testing composite hypotheses. Ann. Math. Statist. **9**, 60 (1938). https://doi.org/10.1214/aoms/1177732360
55. G. Cowan, K. Cranmer, E. Gross, O. Vitells, Asymptotic formulae for likelihood-based tests of new physics. Eur. Phys. J. C **71**, 1554 (2011). https://doi.org/10.1140/epjc/s10052-011-1554-0. arXiv:1007.1727 (Erratum: https://doi.org/10.1140/epjc/s10052-013-2501-z)

CMS Collaboration

Yerevan Physics Institute, Yerevan, Armenia
A. M. Sirunyan, A. Tumasyan

Institut für Hochenergiephysik, Vienna, Austria
W. Adam, F Ambrogi, E. Asilar, T. Bergauer, J. Brandstetter, E. Brondolin, M. Dragicevic, J. Erö, M. Flechl, M. Friedl, R. Frühwirth[1], V. M. Ghete, J. Grossmann, J. Hrubec, M. Jeitler[1], A. König, N. Krammer, I. Krätschmer, D. Liko, T. Madlener, I. Mikulec, E. Pree, D. Rabady, N. Rad, H. Rohringer, J. Schieck[1], R. Schöfbeck, M. Spanring, D. Spitzbart, W. Waltenberger, J. Wittmann, C.-E. Wulz[1], M. Zarucki

Institute for Nuclear Problems, Minsk, Belarus
V. Chekhovsky, V. Mossolov, J. Suarez Gonzalez

Universiteit Antwerpen, Antwerpen, Belgium
E. A. De Wolf, D. Di Croce, X. Janssen, J. Lauwers, M. Van De Klundert, H. Van Haevermaet, P. Van Mechelen, N. Van Remortel

Vrije Universiteit Brussel, Brussel, Belgium
S. Abu Zeid, F. Blekman, J. D'Hondt, I. De Bruyn, J. De Clercq, K. Deroover, G. Flouris, D. Lontkovskyi, S. Lowette, S. Moortgat, L. Moreels, Q. Python, K. Skovpen, S. Tavernier, W. Van Doninck, P. Van Mulders, I. Van Parijs

Université Libre de Bruxelles, Bruxelles, Belgium
H. Brun, B. Clerbaux, G. De Lentdecker, H. Delannoy, G. Fasanella, L. Favart, R. Goldouzian, A. Grebenyuk, G. Karapostoli, T. Lenzi, J. Luetic, T. Maerschalk, A. Marinov, A. Randle-conde, T. Seva, C. Vander Velde, P. Vanlaer, D. Vannerom, R. Yonamine, F. Zenoni, F. Zhang[2]

Ghent University, Ghent, Belgium
A. Cimmino, T. Cornelis, D. Dobur, A. Fagot, M. Gul, I. Khvastunov, D. Poyraz, C. Roskas, S. Salva, M. Tytgat, W. Verbeke, N. Zaganidis

Université Catholique de Louvain, Louvain-la-Neuve, Belgium
H. Bakhshiansohi, O. Bondu, S. Brochet, G. Bruno, C. Caputo, A. Caudron, S. De Visscher, C. Delaere, M. Delcourt, B. Francois, A. Giammanco, A. Jafari, M. Komm, G. Krintiras, V. Lemaitre, A. Magitteri, A. Mertens, M. Musich, K. Piotrzkowski, L. Quertenmont, M. Vidal Marono, S. Wertz

Université de Mons, Mons, Belgium
N. Beliy

Centro Brasileiro de Pesquisas Fisicas, Rio de Janeiro, Brazil
W. L. Aldá Júnior, F. L. Alves, G. A. Alves, L. Brito, M. Correa Martins Junior, C. Hensel, A. Moraes, M. E. Pol, P. Rebello Teles

Universidade do Estado do Rio de Janeiro, Rio de Janeiro, Brazil
E. Belchior Batista Das Chagas, W. Carvalho, J. Chinellato[3], A. Custódio, E. M. Da Costa, G. G. Da Silveira[4], D. De Jesus Damiao, S. Fonseca De Souza, L. M. Huertas Guativa, H. Malbouisson, M. Melo De Almeida, C. Mora Herrera, L. Mundim, H. Nogima, A. Santoro, A. Sznajder, E. J. Tonelli Manganote[3], F. Torres Da Silva De Araujo, A. Vilela Pereira

Universidade Estadual Paulista[a], Universidade Federal do ABC[b], São Paulo, Brazil
S. Ahuja[a], C. A. Bernardes[a], T. R. Fernandez Perez Tomei[a], E. M. Gregores[b], P. G. Mercadante[b], S. F. Novaes[a], Sandra S. Padula[a], D. Romero Abad[b], J. C. Ruiz Vargas[a]

Institute for Nuclear Research and Nuclear Energy, Bulgaria Academy of Sciences, Sofia, Bulgaria
A. Aleksandrov, R. Hadjiiska, P. Iaydjiev, M. Misheva, M. Rodozov, M. Shopova, S. Stoykova, G. Sultanov

University of Sofia, Sofia, Bulgaria
A. Dimitrov, I. Glushkov, L. Litov, B. Pavlov, P. Petkov

Beihang University, Beijing, China
W. Fang[5], X. Gao[5]

Institute of High Energy Physics, Beijing, China
M. Ahmad, J. G. Bian, G. M. Chen, H. S. Chen, M. Chen, Y. Chen, C. H. Jiang, D. Leggat, H. Liao, Z. Liu, F. Romeo, S. M. Shaheen, A. Spiezia, J. Tao, C. Wang, Z. Wang, E. Yazgan, H. Zhang, J. Zhao

State Key Laboratory of Nuclear Physics and Technology, Peking University, Beijing, China
Y. Ban, G. Chen, Q. Li, S. Liu, Y. Mao, S. J. Qian, D. Wang, Z. Xu

Universidad de Los Andes, Bogota, Colombia
C. Avila, A. Cabrera, L. F. Chaparro Sierra, C. Florez, C. F. González Hernández, J. D. Ruiz Alvarez

University of Split, Faculty of Electrical Engineering, Mechanical Engineering and Naval Architecture, Split, Croatia
B. Courbon, N. Godinovic, D. Lelas, I. Puljak, P. M. Ribeiro Cipriano, T. Sculac

University of Split, Faculty of Science, Split, Croatia
Z. Antunovic, M. Kovac

Institute Rudjer Boskovic, Zagreb, Croatia
V. Brigljevic, D. Ferencek, K. Kadija, B. Mesic, A. Starodumov[6], T. Susa

University of Cyprus, Nicosia, Cyprus
M. W. Ather, A. Attikis, G. Mavromanolakis, J. Mousa, C. Nicolaou, F. Ptochos, P. A. Razis, H. Rykaczewski

Charles University, Prague, Czech Republic
M. Finger[7], M. Finger Jr.[7]

Universidad San Francisco de Quito, Quito, Ecuador
E. Carrera Jarrin

Academy of Scientific Research and Technology of the Arab Republic of Egypt, Egyptian Network of High Energy Physics, Cairo, Egypt
Y. Assran[8,9], M. A. Mahmoud[9,10], A. Mahrous[11]

National Institute of Chemical Physics and Biophysics, Tallinn, Estonia
R. K. Dewanjee, M. Kadastik, L. Perrini, M. Raidal, A. Tiko, C. Veelken

Department of Physics, University of Helsinki, Helsinki, Finland
P. Eerola, J. Pekkanen, M. Voutilainen

Helsinki Institute of Physics, Helsinki, Finland
J. Härkönen, T. Järvinen, V. Karimäki, R. Kinnunen, T. Lampén, K. Lassila-Perini, S. Lehti, T. Lindén, P. Luukka, E. Tuominen, J. Tuominiemi, E. Tuovinen

Lappeenranta University of Technology, Lappeenranta, Finland
J. Talvitie, T. Tuuva

IRFU, CEA, Université Paris-Saclay, Gif-sur-Yvette, France
M. Besancon, F. Couderc, M. Dejardin, D. Denegri, J. L. Faure, F. Ferri, S. Ganjour, S. Ghosh, A. Givernaud, P. Gras, G. Hamel de Monchenault, P. Jarry, I. Kucher, E. Locci, M. Machet, J. Malcles, G. Negro, J. Rander, A. Rosowsky, M. Ö. Sahin, M. Titov

Laboratoire Leprince-Ringuet, Ecole Polytechnique, CNRS/IN2P3, Université Paris-Saclay, Palaiseau, France
A. Abdulsalam, I. Antropov, S. Baffioni, F. Beaudette, P. Busson, L. Cadamuro, C. Charlot, R. Granier de Cassagnac, M. Jo, S. Lisniak, A. Lobanov, J. Martin Blanco, M. Nguyen, C. Ochando, G. Ortona, P. Paganini, P. Pigard, S. Regnard, R. Salerno, J. B. Sauvan, Y. Sirois, A. G. Stahl Leiton, T. Strebler, Y. Yilmaz, A. Zabi, A. Zghiche

Université de Strasbourg, CNRS, IPHC UMR 7178, F-67000, Strasbourg, France
J.-L. Agram[12], J. Andrea, D. Bloch, J.-M. Brom, M. Buttignol, E. C. Chabert, N. Chanon, C. Collard, E. Conte[12], X. Coubez, J.-C. Fontaine[12], D. Gelé, U. Goerlach, M. Jansová, A.-C. Le Bihan, N. Tonon, P. Van Hove

Centre de Calcul de l'Institut National de Physique Nucleaire et de Physique des Particules, CNRS/IN2P3, Villeurbanne, France
S. Gadrat

Université de Lyon, Université Claude Bernard Lyon 1, CNRS-IN2P3, Institut de Physique Nucléaire de Lyon, Villeurbanne, France
S. Beauceron, C. Bernet, G. Boudoul, R. Chierici, D. Contardo, P. Depasse, H. El Mamouni, J. Fay, L. Finco, S. Gascon, M. Gouzevitch, G. Grenier, B. Ille, F. Lagarde, I. B. Laktineh, M. Lethuillier, L. Mirabito, A. L. Pequegnot, S. Perries, A. Popov[13], V. Sordini, M. Vander Donckt, S. Viret

Georgian Technical University, Tbilisi, Georgia
A. Khvedelidze[7]

Tbilisi State University, Tbilisi, Georgia
Z. Tsamalaidze[7]

RWTH Aachen University, I. Physikalisches Institut, Aachen, Germany
C. Autermann, S. Beranek, L. Feld, M. K. Kiesel, K. Klein, M. Lipinski, M. Preuten, C. Schomakers, J. Schulz, T. Verlage

RWTH Aachen University, III. Physikalisches Institut A, Aachen, Germany
A. Albert, E. Dietz-Laursonn, D. Duchardt, M. Endres, M. Erdmann, S. Erdweg, T. Esch, R. Fischer, A. Güth, M. Hamer, T. Hebbeker, C. Heidemann, K. Hoepfner, S. Knutzen, M. Merschmeyer, A. Meyer, P. Millet, S. Mukherjee, M. Olschewski, K. Padeken, T. Pook, M. Radziej, H. Reithler, M. Rieger, F. Scheuch, D. Teyssier, S. Thüer

RWTH Aachen University, III. Physikalisches Institut B, Aachen, Germany
G. Flügge, B. Kargoll, T. Kress, A. Künsken, J. Lingemann, T. Müller, A. Nehrkorn, A. Nowack, C. Pistone, O. Pooth, A. Stahl[14]

Deutsches Elektronen-Synchrotron, Hamburg, Germany
M. Aldaya Martin, T. Arndt, C. Asawatangtrakuldee, K. Beernaert, O. Behnke, U. Behrens, A. Bermúdez Martínez, A. A. Bin Anuar, K. Borras[15], V. Botta, A. Campbell, P. Connor, C. Contreras-Campana, F. Costanza, C. Diez Pardos, G. Eckerlin, D. Eckstein, T. Eichhorn, E. Eren, E. Gallo[16], J. Garay Garcia, A. Geiser, A. Gizhko, J. M. Grados Luyando, A. Grohsjean, P. Gunnellini, M. Guthoff, A. Harb, J. Hauk, M. Hempel[17], H. Jung, A. Kalogeropoulos, M. Kasemann, J. Keaveney, C. Kleinwort, I. Korol, D. Krücker, W. Lange, A. Lelek, T. Lenz, J. Leonard, K. Lipka, W. Lohmann[17], R. Mankel, I.-A. Melzer-Pellmann, A. B. Meyer, G. Mittag, J. Mnich, A. Mussgiller, E. Ntomari, D. Pitzl, A. Raspereza, B. Roland, M. Savitskyi, P. Saxena, R. Shevchenko, S. Spannagel, N. Stefaniuk, G. P. Van Onsem, R. Walsh, Y. Wen, K. Wichmann, C. Wissing, O. Zenaiev

University of Hamburg, Hamburg, Germany
S. Bein, V. Blobel, M. Centis Vignali, T. Dreyer, E. Garutti, D. Gonzalez, J. Haller, A. Hinzmann, M. Hoffmann, A. Karavdina, R. Klanner, R. Kogler, N. Kovalchuk, S. Kurz, T. Lapsien, I. Marchesini, D. Marconi, M. Meyer, M. Niedziela, D. Nowatschin, F. Pantaleo[14], T. Peiffer, A. Perieanu, C. Scharf, P. Schleper, A. Schmidt, S. Schumann, J. Schwandt, J. Sonneveld, H. Stadie, G. Steinbrück, F. M. Stober, M. Stöver, H. Tholen, D. Troendle, E. Usai, L. Vanelderen, A. Vanhoefer, B. Vormwald

Institut für Experimentelle Kernphysik, Karlsruhe, Germany
M. Akbiyik, C. Barth, S. Baur, E. Butz, R. Caspart, T. Chwalek, F. Colombo, W. De Boer, A. Dierlamm, B. Freund, R. Friese, M. Giffels, A. Gilbert, D. Haitz, F. Hartmann[14], S. M. Heindl, U. Husemann, F. Kassel[14], S. Kudella, H. Mildner, M. U. Mozer, Th. Müller, M. Plagge, G. Quast, K. Rabbertz, M. Schröder, I. Shvetsov, G. Sieber, H. J. Simonis, R. Ulrich, S. Wayand, M. Weber, T. Weiler, S. Williamson, C. Wöhrmann, R. Wolf

Institute of Nuclear and Particle Physics (INPP), NCSR Demokritos, Aghia Paraskevi, Greece
G. Anagnostou, G. Daskalakis, T. Geralis, V. A. Giakoumopoulou, A. Kyriakis, D. Loukas, I. Topsis-Giotis

National and Kapodistrian University of Athens, Athens, Greece
G. Karathanasis, S. Kesisoglou, A. Panagiotou, N. Saoulidou

National Technical University of Athens, Athens, Greece
K. Kousouris

University of Ioánnina, Ioannina, Greece
I. Evangelou, C. Foudas, P. Kokkas, S. Mallios, N. Manthos, I. Papadopoulos, E. Paradas, J. Strologas, F. A. Triantis

MTA-ELTE Lendület CMS Particle and Nuclear Physics Group, Eötvös Loránd University, Budapest, Hungary
M. Csanad, N. Filipovic, G. Pasztor, G. I. Veres[18]

Wigner Research Centre for Physics, Budapest, Hungary
G. Bencze, C. Hajdu, D. Horvath[19], Á. Hunyadi, F. Sikler, V. Veszpremi, G. Vesztergombi[18], A. J. Zsigmond

Institute of Nuclear Research ATOMKI, Debrecen, Hungary
N. Beni, S. Czellar, J. Karancsi[20], A. Makovec, J. Molnar, Z. Szillasi

Institute of Physics, University of Debrecen, Debrecen, Hungary
M. Bartók[18], P. Raics, Z. L. Trocsanyi, B. Ujvari

Indian Institute of Science (IISc), Bangalore, India
S. Choudhury, J. R. Komaragiri

National Institute of Science Education and Research, Bhubaneswar, India
S. Bahinipati[21], S. Bhowmik, P. Mal, K. Mandal, A. Nayak[22], D. K. Sahoo[21], N. Sahoo, S. K. Swain

Panjab University, Chandigarh, India
S. Bansal, S. B. Beri, V. Bhatnagar, R. Chawla, N. Dhingra, A. K. Kalsi, A. Kaur, M. Kaur, R. Kumar, P. Kumari, A. Mehta, J. B. Singh, G. Walia

University of Delhi, Delhi, India
Ashok Kumar, Aashaq Shah, A. Bhardwaj, S. Chauhan, B. C. Choudhary, R. B. Garg, S. Keshri, A. Kumar, S. Malhotra, M. Naimuddin, K. Ranjan, R. Sharma

Saha Institute of Nuclear Physics, HBNI, Kolkata, India
R. Bhardwaj, R. Bhattacharya, S. Bhattacharya, U. Bhawandeep, S. Dey, S. Dutt, S. Dutta, S. Ghosh, N. Majumdar, A. Modak, K. Mondal, S. Mukhopadhyay, S. Nandan, A. Purohit, A. Roy, D. Roy, S. Roy Chowdhury, S. Sarkar, M. Sharan, S. Thakur

Indian Institute of Technology Madras, Madras, India
P. K. Behera

Bhabha Atomic Research Centre, Mumbai, India
R. Chudasama, D. Dutta, V. Jha, V. Kumar, A. K. Mohanty[14], P. K. Netrakanti, L. M. Pant, P. Shukla, A. Topkar

Tata Institute of Fundamental Research-A, Mumbai, India
T. Aziz, S. Dugad, B. Mahakud, S. Mitra, G. B. Mohanty, N. Sur, B. Sutar

Tata Institute of Fundamental Research-B, Mumbai, India
S. Banerjee, S. Bhattacharya, S. Chatterjee, P. Das, M. Guchait, Sa. Jain, S. Kumar, M. Maity[23], G. Majumder, K. Mazumdar, T. Sarkar[23], N. Wickramage[24]

Indian Institute of Science Education and Research (IISER), Pune, India
S. Chauhan, S. Dube, V. Hegde, A. Kapoor, K. Kothekar, S. Pandey, A. Rane, S. Sharma

Institute for Research in Fundamental Sciences (IPM), Tehran, Iran
S. Chenarani[25], E. Eskandari Tadavani, S. M. Etesami[25], M. Khakzad, M. Mohammadi Najafabadi, M. Naseri, S. Paktinat Mehdiabadi[26], F. Rezaei Hosseinabadi, B. Safarzadeh[27], M. Zeinali

University College Dublin, Dublin, Ireland
M. Felcini, M. Grunewald

INFN Sezione di Bari[a], Università di Bari[b], Politecnico di Bari[c], Bari, Italy
M. Abbrescia[a,b], C. Calabria[a,b], A. Colaleo[a], D. Creanza[a,c], L. Cristella[a,b], N. De Filippis[a,c], M. De Palma[a,b], F. Errico[a,b], L. Fiore[a], G. Iaselli[a,c], S. Lezki[a,b], G. Maggi[a,c], M. Maggi[a], G. Miniello[a,b], S. My[a,b], S. Nuzzo[a,b], A. Pompili[a,b], G. Pugliese[a,c], R. Radogna[a,b], A. Ranieri[a], G. Selvaggi[a,b], A. Sharma[a], L. Silvestris[a,14], R. Venditti[a], P. Verwilligen[a]

INFN Sezione di Bologna[a], Università di Bologna[b], Bologna, Italy
G. Abbiendi[a], C. Battilana[a,b], D. Bonacorsi[a,b], S. Braibant-Giacomelli[a,b], R. Campanini[a,b], P. Capiluppi[a,b], A. Castro[a,b], F. R. Cavallo[a], S. S. Chhibra[a], G. Codispoti[a,b], M. Cuffiani[a,b], G. M. Dallavalle[a], F. Fabbri[a], A. Fanfani[a,b], D. Fasanella[a,b], P. Giacomelli[a], C. Grandi[a], L. Guiducci[a,b], S. Marcellini[a], G. Masetti[a], A. Montanari[a], F. L. Navarria[a,b], A. Perrotta[a], A. M. Rossi[a,b], T. Rovelli[a,b], G. P. Siroli[a,b], N. Tosi[a]

INFN Sezione di Catania[a], Università di Catania[b], Catania, Italy
S. Albergo[a,b], S. Costa[a,b], A. Di Mattia[a], F. Giordano[a,b], R. Potenza[a,b], A. Tricomi[a,b], C. Tuve[a,b]

INFN Sezione di Firenze[a], Università di Firenze[b], Firenze, Italy
G. Barbagli[a], K. Chatterjee[a,b], V. Ciulli[a,b], C. Civinini[a], R. D'Alessandro[a,b], E. Focardi[a,b], P. Lenzi[a,b], M. Meschini[a], S. Paoletti[a], L. Russo[a,28], G. Sguazzoni[a], D. Strom[a], L. Viliani[a,b,14]

INFN Laboratori Nazionali di Frascati, Frascati, Italy
L. Benussi, S. Bianco, F. Fabbri, D. Piccolo, F. Primavera[14]

INFN Sezione di Genova[a], Università di Genova[b], Genova, Italy
V. Calvelli[a,b], F. Ferro[a], E. Robutti[a], S. Tosi[a,b]

INFN Sezione di Milano-Bicocca[a], Università di Milano-Bicocca[b], Milano, Italy
A. Benaglia[a], L. Brianza[a,b], F. Brivio[a,b], V. Ciriolo[a,b], M. E. Dinardo[a,b], S. Fiorendi[a,b], S. Gennai[a], A. Ghezzi[a,b], P. Govoni[a,b], M. Malberti[a,b], S. Malvezzi[a], R. A. Manzoni[a,b], D. Menasce[a], L. Moroni[a], M. Paganoni[a,b], D. Pedrini[a], S. Pigazzini[a,b,29], S. Ragazzi[a,b], T. Tabarelli de Fatis[a,b]

INFN Sezione di Napoli[a], Università di Napoli 'Federico II' [b], Napoli, Italy, Università della Basilicata[c], Potenza, Italy, Università G. Marconi[d], Roma, Italy
S. Buontempo[a], N. Cavallo[a,c], S. Di Guida[a,d,14], F. Fabozzi[a,c], F. Fienga[a,b], A. O. M. Iorio[a,b], W. A. Khan[a], L. Lista[a], S. Meola[a,d,14], P. Paolucci[a,14], C. Sciacca[a,b], F. Thyssen[a]

INFN Sezione di Padova[a], Università di Padova[b], Padova, Italy, Università di Trento[c], Trento, Italy
P. Azzi[a,14], N. Bacchetta[a], L. Benato[a,b], D. Bisello[a,b], A. Boletti[a,b], R. Carlin[a,b], A. Carvalho Antunes De Oliveira[a,b], P. Checchia[a], M. Dall'Osso[a,b], P. De Castro Manzano[a], T. Dorigo[a], U. Dosselli[a], U. Gasparini[a,b], A. Gozzelino[a], S. Lacaprara[a], P. Lujan, M. Margoni[a,b], A. T. Meneguzzo[a,b], N. Pozzobon[a,b], P. Ronchese[a,b], R. Rossin[a,b], F. Simonetto[a,b], E. Torassa[a], S. Ventura[a], M. Zanetti[a,b], P. Zotto[a,b]

INFN Sezione di Pavia[a], Università di Pavia[b], Pavia, Italy
A. Braghieri[a], A. Magnani[a,b], P. Montagna[a,b], S. P. Ratti[a,b], V. Re[a], M. Ressegotti, C. Riccardi[a,b], P. Salvini[a], I. Vai[a,b], P. Vitulo[a,b]

INFN Sezione di Perugia[a], Università di Perugia[b], Perugia, Italy
L. Alunni Solestizi[a,b], M. Biasini[a,b], G. M. Bilei[a], C. Cecchi[a,b], D. Ciangottini[a,b], L. Fanò[a,b], P. Lariccia[a,b], R. Leonardi[a,b], E. Manoni[a], G. Mantovani[a,b], V. Mariani[a,b], M. Menichelli[a], A. Rossi[a,b], A. Santocchia[a,b], D. Spiga[a]

INFN Sezione di Pisa[a], Università di Pisa[b], Scuola Normale Superiore di Pisa[c], Pisa, Italy
K. Androsov[a], P. Azzurri[a,14], G. Bagliesi[a], J. Bernardini[a], T. Boccali[a], L. Borrello, R. Castaldi[a], M. A. Ciocci[a,b], R. Dell'Orso[a], G. Fedi[a], L. Giannini[a,c], A. Giassi[a], M. T. Grippo[a,28], F. Ligabue[a,c], T. Lomtadze[a], E. Manca[a,c], G. Mandorli[a,c], L. Martini[a,b], A. Messineo[a,b], F. Palla[a], A. Rizzi[a,b], A. Savoy-Navarro[a,30], P. Spagnolo[a], R. Tenchini[a], G. Tonelli[a,b], A. Venturi[a], P. G. Verdini[a]

INFN Sezione di Roma[a], Università di Roma[b], Roma, Italy
L. Barone[a,b], F. Cavallari[a], M. Cipriani[a,b], N. Daci[a], D. Del Re[a,b,14], E. Di Marco[a,b], M. Diemoz[a], S. Gelli[a,b], E. Longo[a,b], F. Margaroli[a,b], B. Marzocchi[a,b], P. Meridiani[a], G. Organtini[a,b], R. Paramatti[a,b], F. Preiato[a,b], S. Rahatlou[a,b], C. Rovelli[a], F. Santanastasio[a,b]

INFN Sezione di Torino[a], Università di Torino[b], Turin, Italy, Università del Piemonte Orientale[c], Novara, Italy
N. Amapane[a,b], R. Arcidiacono[a,c], S. Argiro[a,b], M. Arneodo[a,c], N. Bartosik[a], R. Bellan[a,b], C. Biino[a], N. Cartiglia[a], F. Cenna[a,b], M. Costa[a,b], R. Covarelli[a,b], A. Degano[a,b], N. Demaria[a], B. Kiani[a,b], C. Mariotti[a], S. Maselli[a], E. Migliore[a,b], V. Monaco[a,b], E. Monteil[a,b], M. Monteno[a], M. M. Obertino[a,b], L. Pacher[a,b], N. Pastrone[a], M. Pelliccioni[a], G. L. Pinna Angioni[a,b], F. Ravera[a,b], A. Romero[a,b], M. Ruspa[a,c], R. Sacchi[a,b], K. Shchelina[a,b], V. Sola[a], A. Solano[a,b], A. Staiano[a], P. Traczyk[a,b]

INFN Sezione di Trieste[a], Università di Trieste[b], Trieste, Italy
S. Belforte[a], M. Casarsa[a], F. Cossutti[a], G. Della Ricca[a,b], A. Zanetti[a]

Kyungpook National University, Daegu, Korea
D. H. Kim, G. N. Kim, M. S. Kim, J. Lee, S. Lee, S. W. Lee, C. S. Moon, Y. D. Oh, S. Sekmen, D. C. Son, Y. C. Yang

Chonbuk National University, Jeonju, Korea
A. Lee

Chonnam National University, Institute for Universe and Elementary Particles, Kwangju, Korea
H. Kim, D. H. Moon, G. Oh

Hanyang University, Seoul, Korea
J. A. Brochero Cifuentes, J. Goh, T. J. Kim

Korea University, Seoul, Korea
S. Cho, S. Choi, Y. Go, D. Gyun, S. Ha, B. Hong, Y. Jo, Y. Kim, K. Lee, K. S. Lee, S. Lee, J. Lim, S. K. Park, Y. Roh

Seoul National University, Seoul, Korea
J. Almond, J. Kim, J. S. Kim, H. Lee, K. Lee, K. Nam, S. B. Oh, B. C. Radburn-Smith, S. h. Seo, U. K. Yang, H. D. Yoo, G. B. Yu

University of Seoul, Seoul, Korea
M. Choi, H. Kim, J. H. Kim, J. S. H. Lee, I. C. Park

Sungkyunkwan University, Suwon, Korea
Y. Choi, C. Hwang, J. Lee, I. Yu

Vilnius University, Vilnius, Lithuania
V. Dudenas, A. Juodagalvis, J. Vaitkus

National Centre for Particle Physics, Universiti Malaya, Kuala Lumpur, Malaysia
I. Ahmed, Z. A. Ibrahim, M. A. B. Md Ali[31], F. Mohamad Idris[32], W. A. T. Wan Abdullah, M. N. Yusli, Z. Zolkapli

Centro de Investigacion y de Estudios Avanzados del IPN, Mexico City, Mexico
R. Reyes-Almanza, G. Ramirez-Sanchez, M. C. Duran-Osuna, H. Castilla-Valdez, E. De La Cruz-Burelo, I. Heredia-De La Cruz[33], R. I. Rabadan-Trejo, R. Lopez-Fernandez, J. Mejia Guisao, A. Sanchez-Hernandez

Universidad Iberoamericana, Mexico City, Mexico
S. Carrillo Moreno, C. Oropeza Barrera, F. Vazquez Valencia

Benemerita Universidad Autonoma de Puebla, Puebla, Mexico
I. Pedraza, H. A. Salazar Ibarguen, C. Uribe Estrada

Universidad Autónoma de San Luis Potosí, San Luis Potosi, Mexico
A. Morelos Pineda

University of Auckland, Auckland, New Zealand
D. Krofcheck

University of Canterbury, Christchurch, New Zealand
P. H. Butler

National Centre for Physics, Quaid-I-Azam University, Islamabad, Pakistan
A. Ahmad, M. Ahmad, Q. Hassan, H. R. Hoorani, A. Saddique, M. A. Shah, M. Shoaib, M. Waqas

National Centre for Nuclear Research, Swierk, Poland
H. Bialkowska, M. Bluj, B. Boimska, T. Frueboes, M. Górski, M. Kazana, K. Nawrocki, M. Szleper, P. Zalewski

Institute of Experimental Physics, Faculty of Physics, University of Warsaw, Warsaw, Poland
K. Bunkowski, A. Byszuk[34], K. Doroba, A. Kalinowski, M. Konecki, J. Krolikowski, M. Misiura, M. Olszewski, A. Pyskir, M. Walczak

Laboratório de Instrumentação e Física Experimental de Partículas, Lisboa, Portugal
P. Bargassa, C. Beirão Da Cruz E. Silva, A. Di Francesco, P. Faccioli, B. Galinhas, M. Gallinaro, J. Hollar, N. Leonardo, L. Lloret Iglesias, M. V. Nemallapudi, J. Seixas, G. Strong, O. Toldaiev, D. Vadruccio, J. Varela

Joint Institute for Nuclear Research, Dubna, Russia
S. Afanasiev, P. Bunin, M. Gavrilenko, I. Golutvin, I. Gorbunov, A. Kamenev, V. Karjavin, A. Lanev, A. Malakhov, V. Matveev[35,36], V. Palichik, V. Perelygin, S. Shmatov, S. Shulha, N. Skatchkov, V. Smirnov, N. Voytishin, A. Zarubin

Petersburg Nuclear Physics Institute, Gatchina, (St. Petersburg), Russia
Y. Ivanov, V. Kim[37], E. Kuznetsova[38], P. Levchenko, V. Murzin, V. Oreshkin, I. Smirnov, V. Sulimov, L. Uvarov, S. Vavilov, A. Vorobyev

Institute for Nuclear Research, Moscow, Russia
Yu. Andreev, A. Dermenev, S. Gninenko, N. Golubev, A. Karneyeu, M. Kirsanov, N. Krasnikov, A. Pashenkov, D. Tlisov, A. Toropin

Institute for Theoretical and Experimental Physics, Moscow, Russia
V. Epshteyn, V. Gavrilov, N. Lychkovskaya, V. Popov, I. Pozdnyakov, G. Safronov, A. Spiridonov, A. Stepennov, M. Toms, E. Vlasov, A. Zhokin

Moscow Institute of Physics and Technology, Moscow, Russia
T. Aushev, A. Bylinkin[36]

National Research Nuclear University 'Moscow Engineering Physics Institute' (MEPhI), Moscow, Russia
M. Chadeeva[39], P. Parygin, D. Philippov, S. Polikarpov, E. Popova, V. Rusinov

P.N. Lebedev Physical Institute, Moscow, Russia
V. Andreev, M. Azarkin[36], I. Dremin[36], M. Kirakosyan[37], A. Terkulov

Skobeltsyn Institute of Nuclear Physics, Lomonosov Moscow State University, Moscow, Russia
A. Baskakov, A. Belyaev, E. Boos, M. Dubinin[40], L. Dudko, A. Ershov, A. Gribushin, V. Klyukhin, O. Kodolova, I. Lokhtin, I. Miagkov, S. Obraztsov, S. Petrushanko, V. Savrin, A. Snigirev

Novosibirsk State University (NSU), Novosibirsk, Russia
V. Blinov[41], Y. Skovpen[41], D. Shtol[41]

State Research Center of Russian Federation, Institute for High Energy Physics, Protvino, Russia
I. Azhgirey, I. Bayshev, S. Bitioukov, D. Elumakhov, V. Kachanov, A. Kalinin, D. Konstantinov, V. Krychkine, V. Petrov, R. Ryutin, A. Sobol, S. Troshin, N. Tyurin, A. Uzunian, A. Volkov

University of Belgrade, Faculty of Physics and Vinca Institute of Nuclear Sciences, Belgrade, Serbia
P. Adzic[42], P. Cirkovic, D. Devetak, M. Dordevic, J. Milosevic, V. Rekovic

Centro de Investigaciones Energéticas Medioambientales y Tecnológicas (CIEMAT), Madrid, Spain
J. Alcaraz Maestre, M. Barrio Luna, M. Cerrada, N. Colino, B. De La Cruz, A. Delgado Peris, A. Escalante Del Valle, C. Fernandez Bedoya, J. P. Fernández Ramos, J. Flix, M. C. Fouz, P. Garcia-Abia, O. Gonzalez Lopez, S. Goy Lopez, J. M. Hernandez, M. I. Josa, A. Pérez-Calero Yzquierdo, J. Puerta Pelayo, A. Quintario Olmeda, I. Redondo, L. Romero, M. S. Soares, A. Álvarez Fernández

Universidad Autónoma de Madrid, Madrid, Spain
C. Albajar, J. F. de Trocóniz, M. Missiroli, D. Moran

Universidad de Oviedo, Oviedo, Spain
J. Cuevas, C. Erice, J. Fernandez Menendez, I. Gonzalez Caballero, J. R. González Fernández, E. Palencia Cortezon, S. Sanchez Cruz, I. Suárez Andrés, P. Vischia, J. M. Vizan Garcia

Instituto de Física de Cantabria (IFCA), CSIC-Universidad de Cantabria, Santander, Spain
I. J. Cabrillo, A. Calderon, B. Chazin Quero, E. Curras, J. Duarte Campderros, M. Fernandez, J. Garcia-Ferrero, G. Gomez, A. Lopez Virto, J. Marco, C. Martinez Rivero, P. Martinez Ruiz del Arbol, F. Matorras, J. Piedra Gomez, T. Rodrigo, A. Ruiz-Jimeno, L. Scodellaro, N. Trevisani, I. Vila, R. Vilar Cortabitarte

CERN, European Organization for Nuclear Research, Geneva, Switzerland
D. Abbaneo, E. Auffray, P. Baillon, A. H. Ball, D. Barney, M. Bianco, P. Bloch, A. Bocci, C. Botta, T. Camporesi, R. Castello, M. Cepeda, G. Cerminara, E. Chapon, Y. Chen, D. d'Enterria, A. Dabrowski, V. Daponte, A. David, M. De Gruttola, A. De Roeck, M. Dobson, B. Dorney, T. du Pree, M. Dünser, N. Dupont, A. Elliott-Peisert, P. Everaerts, F. Fallavollita, G. Franzoni, J. Fulcher, W. Funk, D. Gigi, K. Gill, F. Glege, D. Gulhan, P. Harris, J. Hegeman, V. Innocente, P. Janot, O. Karacheban[17], J. Kieseler, H. Kirschenmann, V. Knünz, A. Kornmayer[14], M. J. Kortelainen, M. Krammer[1], C. Lange, P. Lecoq, C. Lourenço, M. T. Lucchini, L. Malgeri, M. Mannelli, A. Martelli, F. Meijers, J. A. Merlin, S. Mersi, E. Meschi, P. Milenovic[43], F. Moortgat, M. Mulders, H. Neugebauer, S. Orfanelli, L. Orsini, L. Pape, E. Perez, M. Peruzzi, A. Petrilli, G. Petrucciani, A. Pfeiffer, M. Pierini, A. Racz, T. Reis, F. Riva, G. Rolandi[44], M. Rovere, H. Sakulin, C. Schäfer, C. Schwick, M. Seidel, M. Selvaggi, A. Sharma, P. Silva, P. Sphicas[45], A. Stakia[45], J. Steggemann, M. Stoye, M. Tosi, D. Treille, A. Triossi, A. Tsirou, V. Veckalns[46], M. Verweij, W. D. Zeuner

Paul Scherrer Institut, Villigen, Switzerland
W. Bertl†, L. Caminada[47], K. Deiters, W. Erdmann, R. Horisberger, Q. Ingram, H. C. Kaestli, D. Kotlinski, U. Langenegger, T. Rohe, S. A. Wiederkehr

ETH Zurich - Institute for Particle Physics and Astrophysics (IPA), Zurich, Switzerland
F. Bachmair, L. Bäni, P. Berger, L. Bianchini, B. Casal, G. Dissertori, M. Dittmar, M. Donegà, C. Grab, C. Heidegger, D. Hits, J. Hoss, G. Kasieczka, T. Klijnsma, W. Lustermann, B. Mangano, M. Marionneau, M. T. Meinhard, D. Meister, F. Micheli, P. Musella, F. Nessi-Tedaldi, F. Pandolfi, J. Pata, F. Pauss, G. Perrin, L. Perrozzi, M. Quittnat, M. Reichmann, M. Schönenberger, L. Shchutska, V. R. Tavolaro, K. Theofilatos, M. L. Vesterbacka Olsson, R. Wallny, D. H. Zhu

Universität Zürich, Zurich, Switzerland
T. K. Aarrestad, C. Amsler[48], M. F. Canelli, A. De Cosa, R. Del Burgo, S. Donato, C. Galloni, T. Hreus, B. Kilminster, J. Ngadiuba, D. Pinna, G. Rauco, P. Robmann, D. Salerno, C. Seitz, Y. Takahashi, A. Zucchetta

National Central University, Chung-Li, Taiwan
V. Candelise, T. H. Doan, Sh. Jain, R. Khurana, C. M. Kuo, W. Lin, A. Pozdnyakov, S. S. Yu

National Taiwan University (NTU), Taipei, Taiwan
Arun Kumar, P. Chang, Y. Chao, K. F. Chen, P. H. Chen, F. Fiori, W.-S. Hou, Y. Hsiung, Y. F. Liu, R.-S. Lu, E. Paganis, A. Psallidas, A. Steen, J. f. Tsai

Chulalongkorn University, Faculty of Science, Department of Physics, Bangkok, Thailand
B. Asavapibhop, K. Kovitanggoon, G. Singh, N. Srimanobhas

Çukurova University, Physics Department, Science and Art Faculty, Adana, Turkey
F. Boran, S. Cerci[49], S. Damarseckin, Z. S. Demiroglu, C. Dozen, I. Dumanoglu, S. Girgis, G. Gokbulut, Y. Guler, I. Hos[50], E. E. Kangal[51], O. Kara, A. Kayis Topaksu, U. Kiminsu, M. Oglakci, G. Onengut[52], K. Ozdemir[53], D. Sunar Cerci[49], B. Tali[49], S. Turkcapar, I. S. Zorbakir, C. Zorbilmez

Middle East Technical University, Physics Department, Ankara, Turkey
B. Bilin, G. Karapinar[54], K. Ocalan[55], M. Yalvac, M. Zeyrek

Bogazici University, Istanbul, Turkey
E. Gülmez, M. Kaya[56], O. Kaya[57], S. Tekten, E. A. Yetkin[58]

Istanbul Technical University, Istanbul, Turkey
M. N. Agaras, S. Atay, A. Cakir, K. Cankocak

Institute for Scintillation Materials of National Academy of Science of Ukraine, Kharkov, Ukraine
B. Grynyov

National Scientific Center, Kharkov Institute of Physics and Technology, Kharkov, Ukraine
L. Levchuk, P. Sorokin

University of Bristol, Bristol, UK
R. Aggleton, F. Ball, L. Beck, J. J. Brooke, D. Burns, E. Clement, D. Cussans, O. Davignon, H. Flacher, J. Goldstein, M. Grimes, G. P. Heath, H. F. Heath, J. Jacob, L. Kreczko, C. Lucas, D. M. Newbold[59], S. Paramesvaran, A. Poll, T. Sakuma, S. Seif El Nasr-storey, D. Smith, V. J. Smith

Rutherford Appleton Laboratory, Didcot, UK
K. W. Bell, A. Belyaev[60], C. Brew, R. M. Brown, L. Calligaris, D. Cieri, D. J. A. Cockerill, J. A. Coughlan, K. Harder, S. Harper, E. Olaiya, D. Petyt, C. H. Shepherd-Themistocleous, A. Thea, I. R. Tomalin, T. Williams

Imperial College, London, UK
G. Auzinger, R. Bainbridge, S. Breeze, O. Buchmuller, A. Bundock, S. Casasso, M. Citron, D. Colling, L. Corpe, P. Dauncey, G. Davies, A. De Wit, M. Della Negra, R. Di Maria, A. Elwood, Y. Haddad, G. Hall, G. Iles, T. James, R. Lane, C. Laner, L. Lyons, A.-M. Magnan, S. Malik, L. Mastrolorenzo, T. Matsushita, J. Nash, A. Nikitenko[6], V. Palladino, M. Pesaresi, D. M. Raymond, A. Richards, A. Rose, E. Scott, C. Seez, A. Shtipliyski, S. Summers, A. Tapper, K. Uchida, M. Vazquez Acosta[61], T. Virdee[14], N. Wardle, D. Winterbottom, J. Wright, S. C. Zenz

Brunel University, Uxbridge, UK
J. E. Cole, P. R. Hobson, A. Khan, P. Kyberd, I. D. Reid, P. Symonds, L. Teodorescu, M. Turner

Baylor University, Waco, USA
A. Borzou, K. Call, J. Dittmann, K. Hatakeyama, H. Liu, N. Pastika, C. Smith

Catholic University of America, Washington, DC, USA
R. Bartek, A. Dominguez

The University of Alabama, Tuscaloosa, USA
A. Buccilli, S. I. Cooper, C. Henderson, P. Rumerio, C. West

Boston University, Boston, USA
D. Arcaro, A. Avetisyan, T. Bose, D. Gastler, D. Rankin, C. Richardson, J. Rohlf, L. Sulak, D. Zou

Brown University, Providence, USA
G. Benelli, D. Cutts, A. Garabedian, J. Hakala, U. Heintz, J. M. Hogan, K. H. M. Kwok, E. Laird, G. Landsberg, Z. Mao, M. Narain, J. Pazzini, S. Piperov, S. Sagir, R. Syarif, D. Yu

University of California, Davis, Davis, USA
R. Band, C. Brainerd, D. Burns, M. Calderon De La Barca Sanchez, M. Chertok, J. Conway, R. Conway, P. T. Cox, R. Erbacher, C. Flores, G. Funk, M. Gardner, W. Ko, R. Lander, C. Mclean, M. Mulhearn, D. Pellett, J. Pilot, S. Shalhout, M. Shi, J. Smith, M. Squires, D. Stolp, K. Tos, M. Tripathi, Z. Wang

University of California, Los Angeles, USA
M. Bachtis, C. Bravo, R. Cousins, A. Dasgupta, A. Florent, J. Hauser, M. Ignatenko, N. Mccoll, D. Saltzberg, C. Schnaible, V. Valuev

University of California, Riverside, Riverside, USA
E. Bouvier, K. Burt, R. Clare, J. Ellison, J. W. Gary, S. M. A. Ghiasi Shirazi, G. Hanson, J. Heilman, P. Jandir, E. Kennedy, F. Lacroix, O. R. Long, M. Olmedo Negrete, M. I. Paneva, A. Shrinivas, W. Si, L. Wang, H. Wei, S. Wimpenny, B. R. Yates

University of California, San Diego, La Jolla, USA
J. G. Branson, S. Cittolin, M. Derdzinski, R. Gerosa, B. Hashemi, A. Holzner, D. Klein, G. Kole, V. Krutelyov, J. Letts, I. Macneill, M. Masciovecchio, D. Olivito, S. Padhi, M. Pieri, M. Sani, V. Sharma, S. Simon, M. Tadel, A. Vartak, S. Wasserbaech[62], J. Wood, F. Würthwein, A. Yagil, G. Zevi Della Porta

University of California, Santa Barbara-Department of Physics, Santa Barbara, USA
N. Amin, R. Bhandari, J. Bradmiller-Feld, C. Campagnari, A. Dishaw, V. Dutta, M. Franco Sevilla, C. George, F. Golf, L. Gouskos, J. Gran, R. Heller, J. Incandela, S. D. Mullin, A. Ovcharova, H. Qu, J. Richman, D. Stuart, I. Suarez, J. Yoo

California Institute of Technology, Pasadena, USA
D. Anderson, J. Bendavid, A. Bornheim, J. M. Lawhorn, H. B. Newman, T. Nguyen, C. Pena, M. Spiropulu, J. R. Vlimant, S. Xie, Z. Zhang, R. Y. Zhu

Carnegie Mellon University, Pittsburgh, USA
M. B. Andrews, T. Ferguson, T. Mudholkar, M. Paulini, J. Russ, M. Sun, H. Vogel, I. Vorobiev, M. Weinberg

University of Colorado Boulder, Boulder, USA
J. P. Cumalat, W. T. Ford, F. Jensen, A. Johnson, M. Krohn, S. Leontsinis, T. Mulholland, K. Stenson, S. R. Wagner

Cornell University, Ithaca, USA
J. Alexander, J. Chaves, J. Chu, S. Dittmer, K. Mcdermott, N. Mirman, J. R. Patterson, A. Rinkevicius, A. Ryd, L. Skinnari, L. Soffi, S. M. Tan, Z. Tao, J. Thom, J. Tucker, P. Wittich, M. Zientek

Fermi National Accelerator Laboratory, Batavia, USA
S. Abdullin, M. Albrow, G. Apollinari, A. Apresyan, A. Apyan, S. Banerjee, L. A. T. Bauerdick, A. Beretvas, J. Berryhill, P. C. Bhat, G. Bolla†, K. Burkett, J. N. Butler, A. Canepa, G. B. Cerati, H. W. K. Cheung, F. Chlebana, M. Cremonesi, J. Duarte, V. D. Elvira, J. Freeman, Z. Gecse, E. Gottschalk, L. Gray, D. Green, S. Grünendahl, O. Gutsche, R. M. Harris, S. Hasegawa, J. Hirschauer, Z. Hu, B. Jayatilaka, S. Jindariani, M. Johnson, U. Joshi, B. Klima, B. Kreis, S. Lammel, D. Lincoln, R. Lipton, M. Liu, T. Liu, R. Lopes De Sá, J. Lykken, K. Maeshima, N. Magini, J. M. Marraffino, S. Maruyama, D. Mason, P. McBride, P. Merkel, S. Mrenna, S. Nahn, V. O'Dell, K. Pedro, O. Prokofyev, G. Rakness, L. Ristori, B. Schneider, E. Sexton-Kennedy, A. Soha, W. J. Spalding, L. Spiegel, S. Stoynev, J. Strait, N. Strobbe, L. Taylor, S. Tkaczyk, N. V. Tran, L. Uplegger, E. W. Vaandering, C. Vernieri, M. Verzocchi, R. Vidal, M. Wang, H. A. Weber, A. Whitbeck

University of Florida, Gainesville, USA
D. Acosta, P. Avery, P. Bortignon, D. Bourilkov, A. Brinkerhoff, A. Carnes, M. Carver, D. Curry, R. D. Field, I. K. Furic, J. Konigsberg, A. Korytov, K. Kotov, P. Ma, K. Matchev, H. Mei, G. Mitselmakher, D. Rank, D. Sperka, N. Terentyev, L. Thomas, J. Wang, S. Wang, J. Yelton

Florida International University, Miami, USA
Y. R. Joshi, S. Linn, P. Markowitz, J. L. Rodriguez

Florida State University, Tallahassee, USA
A. Ackert, T. Adams, A. Askew, S. Hagopian, V. Hagopian, K. F. Johnson, T. Kolberg, G. Martinez, T. Perry, H. Prosper, A. Saha, A. Santra, V. Sharma, R. Yohay

Florida Institute of Technology, Melbourne, USA
M. M. Baarmand, V. Bhopatkar, S. Colafranceschi, M. Hohlmann, D. Noonan, T. Roy, F. Yumiceva

University of Illinois at Chicago (UIC), Chicago, USA
M. R. Adams, L. Apanasevich, D. Berry, R. R. Betts, R. Cavanaugh, X. Chen, O. Evdokimov, C. E. Gerber, D. A. Hangal, D. J. Hofman, K. Jung, J. Kamin, I. D. Sandoval Gonzalez, M. B. Tonjes, H. Trauger, N. Varelas, H. Wang, Z. Wu, J. Zhang

The University of Iowa, Iowa City, USA
B. Bilki[63], W. Clarida, K. Dilsiz[64], S. Durgut, R. P. Gandrajula, M. Haytmyradov, V. Khristenko, J.-P. Merlo, H. Mermerkaya[65], A. Mestvirishvili, A. Moeller, J. Nachtman, H. Ogul[66], Y. Onel, F. Ozok[67], A. Penzo, C. Snyder, E. Tiras, J. Wetzel, K. Yi

Johns Hopkins University, Baltimore, USA
B. Blumenfeld, A. Cocoros, N. Eminizer, D. Fehling, L. Feng, A. V. Gritsan, P. Maksimovic, J. Roskes, U. Sarica, M. Swartz, M. Xiao, C. You

The University of Kansas, Lawrence, USA
A. Al-bataineh, P. Baringer, A. Bean, S. Boren, J. Bowen, J. Castle, S. Khalil, A. Kropivnitskaya, D. Majumder, W. Mcbrayer, M. Murray, C. Royon, S. Sanders, E. Schmitz, R. Stringer, J. D. Tapia Takaki, Q. Wang

Kansas State University, Manhattan, USA
A. Ivanov, K. Kaadze, Y. Maravin, A. Mohammadi, L. K. Saini, N. Skhirtladze, S. Toda

Lawrence Livermore National Laboratory, Livermore, USA
F. Rebassoo, D. Wright

University of Maryland, College Park, USA
C. Anelli, A. Baden, O. Baron, A. Belloni, B. Calvert, S. C. Eno, C. Ferraioli, N. J. Hadley, S. Jabeen, G. Y. Jeng, R. G. Kellogg, J. Kunkle, A. C. Mignerey, F. Ricci-Tam, Y. H. Shin, A. Skuja, S. C. Tonwar

Massachusetts Institute of Technology, Cambridge, USA
D. Abercrombie, B. Allen, V. Azzolini, R. Barbieri, A. Baty, R. Bi, S. Brandt, W. Busza, I. A. Cali, M. D'Alfonso, Z. Demiragli, G. Gomez Ceballos, M. Goncharov, D. Hsu, Y. Iiyama, G. M. Innocenti, M. Klute, D. Kovalskyi, Y. S. Lai, Y.-J. Lee, A. Levin, P. D. Luckey, B. Maier, A. C. Marini, C. Mcginn, C. Mironov, S. Narayanan, X. Niu, C. Paus, C. Roland, G. Roland, J. Salfeld-Nebgen, G. S. F. Stephans, K. Tatar, D. Velicanu, J. Wang, T. W. Wang, B. Wyslouch

University of Minnesota, Minneapolis, USA
A. C. Benvenuti, R. M. Chatterjee, A. Evans, P. Hansen, S. Kalafut, Y. Kubota, Z. Lesko, J. Mans, S. Nourbakhsh, N. Ruckstuhl, R. Rusack, J. Turkewitz

University of Mississippi, Oxford, USA
J. G. Acosta, S. Oliveros

University of Nebraska-Lincoln, Lincoln, USA
E. Avdeeva, K. Bloom, D. R. Claes, C. Fangmeier, R. Gonzalez Suarez, R. Kamalieddin, I. Kravchenko, J. Monroy, J. E. Siado, G. R. Snow, B. Stieger

State University of New York at Buffalo, Buffalo, USA
M. Alyari, J. Dolen, A. Godshalk, C. Harrington, I. Iashvili, D. Nguyen, A. Parker, S. Rappoccio, B. Roozbahani

Northeastern University, Boston, USA
G. Alverson, E. Barberis, A. Hortiangtham, A. Massironi, D. M. Morse, D. Nash, T. Orimoto, R. Teixeira De Lima, D. Trocino, D. Wood

Northwestern University, Evanston, USA
S. Bhattacharya, O. Charaf, K. A. Hahn, N. Mucia, N. Odell, B. Pollack, M. H. Schmitt, K. Sung, M. Trovato, M. Velasco

University of Notre Dame, Notre Dame, USA
N. Dev, M. Hildreth, K. Hurtado Anampa, C. Jessop, D. J. Karmgard, N. Kellams, K. Lannon, N. Loukas, N. Marinelli, F. Meng, C. Mueller, Y. Musienko[35], M. Planer, A. Reinsvold, R. Ruchti, G. Smith, S. Taroni, M. Wayne, M. Wolf, A. Woodard

The Ohio State University, Columbus, USA
J. Alimena, L. Antonelli, B. Bylsma, L. S. Durkin, S. Flowers, B. Francis, A. Hart, C. Hill, W. Ji, B. Liu, W. Luo, D. Puigh, B. L. Winer, H. W. Wulsin

Princeton University, Princeton, USA
S. Cooperstein, O. Driga, P. Elmer, J. Hardenbrook, P. Hebda, S. Higginbotham, D. Lange, J. Luo, D. Marlow, K. Mei, I. Ojalvo, J. Olsen, C. Palmer, P. Piroué, D. Stickland, C. Tully

University of Puerto Rico, Mayaguez, USA
S. Malik, S. Norberg

Purdue University, West Lafayette, USA
A. Barker, V. E. Barnes, S. Das, S. Folgueras, L. Gutay, M. K. Jha, M. Jones, A. W. Jung, A. Khatiwada, D. H. Miller, N. Neumeister, C. C. Peng, J. F. Schulte, J. Sun, F. Wang, W. Xie

Purdue University Northwest, Hammond, USA
T. Cheng, N. Parashar, J. Stupak

Rice University, Houston, USA
A. Adair, B. Akgun, Z. Chen, K. M. Ecklund, F. J. M. Geurts, M. Guilbaud, W. Li, B. Michlin, M. Northup, B. P. Padley, J. Roberts, J. Rorie, Z. Tu, J. Zabel

University of Rochester, Rochester, USA
A. Bodek, P. de Barbaro, R. Demina, Y. t. Duh, T. Ferbel, M. Galanti, A. Garcia-Bellido, J. Han, O. Hindrichs, A. Khukhunaishvili, K. H. Lo, P. Tan, M. Verzetti

The Rockefeller University, New York, USA
R. Ciesielski, K. Goulianos, C. Mesropian

Rutgers, The State University of New Jersey, Piscataway, USA
A. Agapitos, J. P. Chou, Y. Gershtein, T. A. Gómez Espinosa, E. Halkiadakis, M. Heindl, E. Hughes, S. Kaplan, R. Kunnawalkam Elayavalli, S. Kyriacou, A. Lath, R. Montalvo, K. Nash, M. Osherson, H. Saka, S. Salur, S. Schnetzer, D. Sheffield, S. Somalwar, R. Stone, S. Thomas, P. Thomassen, M. Walker

University of Tennessee, Knoxville, USA
A. G. Delannoy, M. Foerster, J. Heideman, G. Riley, K. Rose, S. Spanier, K. Thapa

Texas A & M University, College Station, USA
O. Bouhali[68], A. Castaneda Hernandez[68], A. Celik, M. Dalchenko, M. De Mattia, A. Delgado, S. Dildick, R. Eusebi, J. Gilmore, T. Huang, T. Kamon[69], R. Mueller, Y. Pakhotin, R. Patel, A. Perloff, L. Perniè, D. Rathjens, A. Safonov, A. Tatarinov, K. A. Ulmer

Texas Tech University, Lubbock, USA
N. Akchurin, J. Damgov, F. De Guio, P. R. Dudero, J. Faulkner, E. Gurpinar, S. Kunori, K. Lamichhane, S. W. Lee, T. Libeiro, T. Peltola, S. Undleeb, I. Volobouev, Z. Wang

Vanderbilt University, Nashville, USA
S. Greene, A. Gurrola, R. Janjam, W. Johns, C. Maguire, A. Melo, H. Ni, P. Sheldon, S. Tuo, J. Velkovska, Q. Xu

University of Virginia, Charlottesville, USA
M. W. Arenton, P. Barria, B. Cox, R. Hirosky, A. Ledovskoy, H. Li, C. Neu, T. Sinthuprasith, Y. Wang, E. Wolfe, F. Xia

Wayne State University, Detroit, USA
R. Harr, P. E. Karchin, J. Sturdy, S. Zaleski

University of Wisconsin-Madison, Madison, WI, USA
M. Brodski, J. Buchanan, C. Caillol, S. Dasu, L. Dodd, S. Duric, B. Gomber, M. Grothe, M. Herndon, A. Hervé, U. Hussain, P. Klabbers, A. Lanaro, A. Levine, K. Long, R. Loveless, G. A. Pierro, G. Polese, T. Ruggles, A. Savin, N. Smith, W. H. Smith, D. Taylor, N. Woods

† **Deceased**

1: Also at Vienna University of Technology, Vienna, Austria
2: Also at State Key Laboratory of Nuclear Physics and Technology, Peking University, Beijing, China
3: Also at Universidade Estadual de Campinas, Campinas, Brazil
4: Also at Universidade Federal de Pelotas, Pelotas, Brazil
5: Also at Université Libre de Bruxelles, Bruxelles, Belgium
6: Also at Institute for Theoretical and Experimental Physics, Moscow, Russia
7: Also at Joint Institute for Nuclear Research, Dubna, Russia
8: Also at Suez University, Suez, Egypt
9: Now at British University in Egypt, Cairo, Egypt
10: Also at Fayoum University, El-Fayoum, Egypt
11: Now at Helwan University, Cairo, Egypt
12: Also at Université de Haute Alsace, Mulhouse, France
13: Also at Skobeltsyn Institute of Nuclear Physics, Lomonosov Moscow State University, Moscow, Russia
14: Also at CERN, European Organization for Nuclear Research, Geneva, Switzerland
15: Also at RWTH Aachen University, III. Physikalisches Institut A, Aachen, Germany

16: Also at University of Hamburg, Hamburg, Germany
17: Also at Brandenburg University of Technology, Cottbus, Germany
18: Also at MTA-ELTE Lendület CMS Particle and Nuclear Physics Group, Eötvös Loránd University, Budapest, Hungary
19: Also at Institute of Nuclear Research ATOMKI, Debrecen, Hungary
20: Also at Institute of Physics, University of Debrecen, Debrecen, Hungary
21: Also at Indian Institute of Technology Bhubaneswar, Bhubaneswar, India
22: Also at Institute of Physics, Bhubaneswar, India
23: Also at University of Visva-Bharati, Santiniketan, India
24: Also at University of Ruhuna, Matara, Sri Lanka
25: Also at Isfahan University of Technology, Isfahan, Iran
26: Also at Yazd University, Yazd, Iran
27: Also at Plasma Physics Research Center, Science and Research Branch, Islamic Azad University, Tehran, Iran
28: Also at Università degli Studi di Siena, Siena, Italy
29: Also at INFN Sezione di Milano-Bicocca; Università di Milano-Bicocca, Milano, Italy
30: Also at Purdue University, West Lafayette, USA
31: Also at International Islamic University of Malaysia, Kuala Lumpur, Malaysia
32: Also at Malaysian Nuclear Agency, MOSTI, Kajang, Malaysia
33: Also at Consejo Nacional de Ciencia y Tecnología, Mexico city, Mexico
34: Also at Warsaw University of Technology, Institute of Electronic Systems, Warsaw, Poland
35: Also at Institute for Nuclear Research, Moscow, Russia
36: Now at National Research Nuclear University 'Moscow Engineering Physics Institute' (MEPhI), Moscow, Russia
37: Also at St. Petersburg State Polytechnical University, St. Petersburg, Russia
38: Also at University of Florida, Gainesville, USA
39: Also at P.N. Lebedev Physical Institute, Moscow, Russia
40: Also at California Institute of Technology, Pasadena, USA
41: Also at Budker Institute of Nuclear Physics, Novosibirsk, Russia
42: Also at Faculty of Physics, University of Belgrade, Belgrade, Serbia
43: Also at University of Belgrade, Faculty of Physics and Vinca Institute of Nuclear Sciences, Belgrade, Serbia
44: Also at Scuola Normale e Sezione dell'INFN, Pisa, Italy
45: Also at National and Kapodistrian University of Athens, Athens, Greece
46: Also at Riga Technical University, Riga, Latvia
47: Also at Universität Zürich, Zurich, Switzerland
48: Also at Stefan Meyer Institute for Subatomic Physics, (SMI), Vienna, Austria
49: Also at Adiyaman University, Adiyaman, Turkey
50: Also at Istanbul Aydin University, Istanbul, Turkey
51: Also at Mersin University, Mersin, Turkey
52: Also at Cag University, Mersin, Turkey
53: Also at Piri Reis University, Istanbul, Turkey
54: Also at Izmir Institute of Technology, Izmir, Turkey
55: Also at Necmettin Erbakan University, Konya, Turkey
56: Also at Marmara University, Istanbul, Turkey
57: Also at Kafkas University, Kars, Turkey
58: Also at Istanbul Bilgi University, Istanbul, Turkey
59: Also at Rutherford Appleton Laboratory, Didcot, UK
60: Also at School of Physics and Astronomy, University of Southampton, Southampton, UK
61: Also at Instituto de Astrofísica de Canarias, La Laguna, Spain
62: Also at Utah Valley University, Orem, USA
63: Also at USABeykent University, Istanbul, Turkey
64: Also at Bingol University, Bingol, Turkey
65: Also at Erzincan University, Erzincan, Turkey
66: Also at Sinop University, Sinop, Turkey

67: Also at Mimar Sinan University, Istanbul, Istanbul, Turkey
68: Also at Texas A&M University at Qatar, Doha, Qatar
69: Also at Kyungpook National University, Taegu, Korea